Palacký University Olomouc,

Faculty of Science, Department of Geoinformatics

Paris Lodron University Salzburg,

Faculty of Digital and Analytical Sciences, Department of Geoinformatics

PORTRAYAL OF LIKELY CLIMATE CHANGE IMPACTS ON BEEKEEPING BASED ON EARTH OBSERVATION DATA

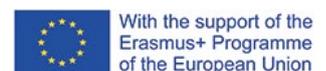**Diploma thesis**

Author

Yuan WANG

Supervisor (Palacký University Olomouc)

RNDr. Jan BRUS, Ph.D.

Co-supervisor (Paris Lodron University Salzburg)

Assoc. Prof. Stefan LANG, Ph.D.

Erasmus Mundus Joint Master Degree Programme
Copernicus Master in Digital Earth
Specialization Track Geovisualization & Geocommunication
Olomouc, Czech Republic, 2022

ANNOTATION

This study focuses on evaluating the potential and limitations of earth observation data in the context of likely climate change and beekeeping support. The study area for the first part of the analysis is the European continent, where the pattern of likely climate change is investigated and visualized using multidimensional raster data of temperature and precipitation obtained from Earth observations. Trend analysis was applied to both annual average temperature and yearly total precipitation from 1950 to 2021 in Europe. The spatial pattern of the changing trend of these two variables is visualized, which not only gives an overview of where and how the climate has changed in Europe but also offers bee experts and beekeepers valuable reference information in the decision-making process that can benefit beekeeping and bee conservation. A before-after comparison for the annual average temperature over the 72 years has also been visualized based on the results from the multidimensional principal components analysis. The relation between likely climate change and the survival of bees is explored at a regional scale (in this case, the national territory of the Czech Republic) as a case study due to the limitations in bee data availability. Regression analysis was carried out between bee colony winter losses and the slope value of trend lines for both temperature and precipitation, respectively. Although the current study design did not reveal statistically relevant correlations, the methodology applied in the analysis can still provide a new perspective for the research of likely climate change impacts on beekeeping. Moreover, similar patterns of fluctuation were observed from the evolution of bee colony winter loss and temperature anomalies over time, which indicates that high bee colony winter loss might be related to high temperature anomalies. In addition to the analysis mentioned above, a web application "EO4BEE" powered by Google Earth Engine was developed to facilitate the visualization of earth observation variables that are crucial to bee health.

KEYWORDS

Climate change, Earth observation, beekeeping, Google Earth Engine, multidimensional raster analysis

Number of pages: 54

Number of appendixes: 3

DECLARATION

This thesis has been composed by Yuan Wang for the Erasmus Mundus Joint Master's Degree Program in Copernicus Master in Digital Earth for the academic year 2021/2022 at the Department of Geoinformatics, Faculty of Natural Sciences, Paris Lodron University Salzburg, and Department of Geoinformatics, Faculty of Digital and Analytical Sciences, Palacký University Olomouc.

Hereby, I declare that this piece of work is entirely my own, the references cited have been acknowledged and the thesis has not been previously submitted to the fulfillment of the higher degree.

12.05.2021, Olomouc   Yuan Wang

ACKNOWLEDGEMENT

Palacký University Olomouc
Faculty of Science
Academic year: 2021/2022

ASSIGNMENT OF DIPLOMA THESIS
(project, art work, art performance)

Name and surname: **Yuan WANG**
Personal number: **R200689**
Study programme: **N0532A330010 Geoinformatics and Cartography**
Work topic: **Portrayal of likely Climate Change Impacts on Beekeeping based on Earth Observation Data**
Assigning department: **Department of Geoinformatics**

Theses guidelines

This study aims to process Earth observation data in the context of beekeeping and likely climate change within Europe and integrate the products and results into a data-powered web application. The student will explore the possibility of integrating several data sources from Earth Observation with crowdsourced information from beekeepers based on the citizen science approach. The second aim is to evaluate the benefits and limitations of available datasets for beekeeping support. The result will be a web application, maps, graphs, and animations. The student will attach all the collected datasets and all the animations to the thesis in digital form. The student will create a website about the thesis following the rules available on the department's website and a poster about the diploma thesis in A2 format. The student will submit the entire text (text, attachments, poster, outputs, input and output data) in digital form on a storage medium and the text of the thesis in two bound copies to the department secretary.

Extent of work report: max. 50 pages
Extent of graphics content: as needed
Form processing of diploma thesis: printed
Language of elaboration: English

Recommended resources:

Rapp, J. R., Lenske, V., Solomon, E., & Young, R. (2018, December). Incorporating NASA Earth Observations into an Assessment Tool to Identify Correlations Between Factors Associated with Bee Health. In AGU Fall Meeting Abstracts (Vol. 2018, pp. GC43I-1643).
Vizcarra, N. Clues in the nectar. (2010). Sensing Our Planet, 34.
Gorelick, N., Hancher, M., Dixon, M., Ilyushchenko, S., Thau, D., & Moore, R. (2017). Google Earth Engine: Planetary-scale geospatial analysis for everyone. Remote sensing of Environment, 202, 18-27.
Kumar, L., & Mutanga, O. (2018). Google Earth Engine applications since inception: Usage, trends, and potential. Remote Sensing, 10(10), 1509.
Amani, M., Ghorbanian, A., Ahmadi, S. A., Kakooei, M., Moghimi, A., Mirmazloumi, S. M., ... & Brisco, B. (2020). Google earth engine cloud computing platform for remote sensing big data applications: A comprehensive review. IEEE Journal of Selected Topics in Applied Earth Observations and Remote Sensing, 13, 5326-5350.
Huntington, J. L., Hegewisch, K. C., Daudert, B., Morton, C. G., Abatzoglou, J. T., McEvoy, D. J., & Erickson, T. (2017). Climate engine: Cloud computing and visualization of climate and remote sensing data for advanced natural resource monitoring and process understanding. Bulletin of the American Meteorological Society, 98(11), 2397-2410.

Supervisors of diploma thesis: RNDr. Jan Brus, Ph.D.
Department of Geoinformatics

Date of assignment of diploma thesis: **December 9, 2021**
Submission deadline of diploma thesis: **May 5, 2022**

L.S.

UNIVERZITA PALACKÉHO V OLOMOUCI
PŘÍRODOVĚDECKÁ FAKULTA
KATEDRA GEOINFORMATIKY
17. listopadu 50, 771 46 Olomouc

_____
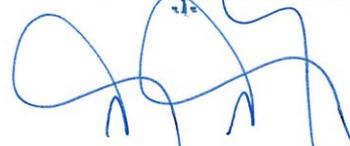
doc. RNDr. Martin Kubala, Ph.D.
Dean

_____

prof. RNDr. Vít Voženílek, CSc.
Head of Department

Olomouc   December 16, 2021

CONTENT

LIST OF ABBREVIATIONS

Abbreviation	Meaning
ABH	Africanized Honey Bee
AVHRR	Advanced Very High Resolution Radiometer
C. australensis	Centris australensis
CRF	Cloud Raster Format
COLOSS	prevention of honey bee COlony LOSSes
C. sponsa	Centris sponsa
E. marianae	Euglossa marianae
EO	Earth Observation
EVI	Enhanced Vegetation Index
GEE	Google Earth Engine
GHG	Green House Gas
GIS	Geographic Information System
GSFC	Goddard Space Flight Center
HBNF	Honey Bee Nectar Flow
IPCC	Intergovernmental Panel on Climate Change
IUCN	International Union for Conservation of Nature
LCZ	Local Climate Zone
LiDAR	Light Detection and Ranging
MODIS	Moderate Resolution Imaging Spectro radiator
NASA	The National Aeronautics and Space Administration
NCEP	National Center for Environmental Prediction
NDVI	Normalized Difference Vegetation Index
PaaS	Platform as a Service
Radar	Radio detection and ranging
RF	Random Forest
USA	United States of America
USDA	U.S. Department of Agriculture

INTRODUCTION

Bees (*Apis*), as one of the most important pollinators in nature, are of significant economic and ecological value, contributing a lot to both global food safety and the maintenance of rich biodiversity. According to the report from the International Union for Conservation of Nature (IUCN), 78% of floral resources and 84% of crops in the European Union rely partially or fully on animal pollination, of which bees account for the majority. However, many scientific researchers and international associations have reported a concerning reduction in the health of the bee population. For instance, over 9% of European bee species are reported by the IUCN to face the risk of extinction (Nieto, 2014), and multiple surveys in Europe (Bommarco et al., 2012; Rasmont et al., 2015) have revealed a decline in distribution and population of many bee species over the course of this century (Cameron & Sadd, 2020). All these findings point to the urgency and necessity to study the reasons behind the bee crisis. Fundamental studies dedicated to exploring the causes of death and effects of human-induced environmental change will be required to understand the reasons favoring bee population reduction.

The causes for the decline mentioned previously can be based on habitat loss, pesticide use, invasive species, climate change, etc. (Brown & Paxton, 2009). And among all these factors, this study focuses on evaluating the patterns of climate change as a factor that might affect bee abundance since climate change has become a growing concern on a planetary scale. The change in climate conditions can affect the survival of bees in many ways: it can influence the behavior and physiology of bees directly, have an indirect impact by changing the phenology of floral resources, or affect the disease profiles and incidence of bees (Le Conte & Navajas, 2008).

Although there have been quite a few studies about the influence of climate change on beekeeping, e.g., Schmickl et al. (2017) analyzed how climate conditions like temperature and precipitation influence honey bee mortality, and Flores et al. (2019) evaluated the effect of climate change on bee colonies. Most of these studies are carried out at a local scale based on conventional data collection methods, which is an enormous endeavor with inherent limitations, considering the fact that the bee crisis is happening on a global scale. In fact, the advancement of EO technologies could fill this research gap effortlessly due to its nature of global coverage and massive data volume, whereas the application of EO data in the context of likely climate change and beekeeping support stays fairly understudied. The reason could be that many bee experts specialize in entomology or biology and have very little knowledge of the latest advances in remote sensing science. With these problems being stated, this diploma thesis aims to provide new insights into how EO data can be used to benefit the current situation of bees, to give bee experts an overview of the methodologies that can be applied to analyze EO datasets related to bee health and to reveal the possibilities of breaking through the limitations of traditional research in terms of spatial and temporal scale.

1 OBJECTIVES

This diploma thesis aims to explore the potential of Earth Observation (EO) data in the context of likely climate change and beekeeping support and to develop a web application powered by EO data that is relevant to the survival of bees. The methodological goals of the analysis part of this study are:

(1) Analyzing the patterns of climate change in Europe using multidimensional raster data obtained from EO technologies;

(2) Investigating the possibility of integrating EO data related to likely climate change and crowdsourced bee colony data from beekeepers in the Czech Republic;

(3) Evaluating how the analysis results from (1) and (2) can assist the decision-making process of beekeepers and bee experts;

The practical goal of this study is to develop a data-powered web application for beekeeping support in concerns of likely climate change. The web application is expected to enable the visualization of EO variables that are crucial to the living environment of bees in a way that the user should be able to browse through the time series of these variables to have an overview of their change pattern.

The results of this study are supposed to provide inspiration from the perspective of EO technologies for the research on the likely impacts of climate change on beekeeping. The methodologies proposed in this study can be easily applied to other regions and time periods, providing bee experts with a detailed reference at a local scale so that they are able to make better decisions that benefit bee survival.

2 METHODOLOGY

2.1 Study area

The study area for the evaluation of climate change is the entire European continent, which is part of the Eurasian continent and located to the west of Asia, with its west, north, and south sides bordered by the Atlantic Ocean, the Arctic Ocean, and the Mediterranean Sea respectively. Most parts of the European continent are located in the mid-latitudes of the north temperate zone and belong to one of the belts of westerly winds in the atmospheric circulation system. Therefore, the climate there is heavily influenced by the Atlantic Ocean, dominated by a temperate oceanic climate that is mild and humid throughout the year. And the study area for the assessment of climate change impacts on beekeeping is the Czech Republic (highlighted in the map), which is located in central Europe.

Figure 1 Geographical overview of the European continent

2.2 Data sources

Data sources for the web application

Information including name, provider, resolution, and time availability of all the EO datasets used for the development of the web application in this study are listed in the table in attachment 1. All of these datasets are easily available in the GEE open data catalog, which is ready for visualization and further analysis.

Data sources for the analysis

The multidimensional raster used for the assessment of climate change in Europe is the ERA5-Land monthly averaged reanalysis dataset with a spatial resolution of 0.1 degree, which is also publicly accessible from the Copernicus climate change service (Muñoz-Sabater, 2019).

Beekeeping data

Except for these datasets obtained from EO technologies, the data of honey bee colony losses is also used to assess the potential effect of likely climate change on beekeeping. The beekeeping data are based on COLOSS monitoring and contains the percentage losses of bee colony, number of wintered colonies and number of lost colonies. Based on colonies density data from Ministry of Agriculture of the Czech Republic the representativeness from 2013 to 2020 for each administrative division with a unique ZIP code in the Czech Republic was calculated. The percentage losses are calculated from the number of wintered colonies and the number of dead colonies within the region of given ZIP code. The representativeness for each year is calculated using the data of the number of beehives provided by the Ministry of Agriculture of the Czech Republic. The dataset is available in shapefile format in the attachment.

2.3 Software and programming languages

Multiple types of software, platforms, as well as programming languages and packages were used in this study, including both open-source and commercial ones. Details on the version and usage of these tools involved in this study are listed in Table 1.

Table 1 Software, platforms, and programming languages/packages

Platform/Software/Programming languages and packages	Version	Usage
Google Earth Engine	/	Provide multi-sourced EO data service; Support back-end computing of the web app
Anaconda	4.10.3	Python package management and deployment
Jupyter Notebook	6.4.6	IDE for the development of the web app
Python	3.8.8	Development of the web app
geemap	0.12.0	
earthengine-api	0.1.303	
Voila	0.3.0	
httplib2	0.19.1	
Heroku CLI	7.53.0	Platform as a service (PaaS) for hosting the web app in the cloud
ArcGIS Pro	2.9.2	Multidimensional raster analysis; Visualization of the final result
JavaScript	ES6	Scripting in the GEE platforms to access relevant dataset

2.4 Workflow

The methodology of this study can basically be explained by the workflow in Figure 2. First and foremost, datasets with variables that have a relatively notable impact on the living environment of bees need to be sifted out from countless EO datasets and then fed into the web application for beekeeping support. These filtered datasets are then visualized in an interactive way in the web application, allowing the beekeepers, bee experts, and enthusiasts to inspect the climate conditions, which are essential to the survival of bees not only at a large spatial scale but also on a long time period. The output of this web application, together with the raw data from earth observations, can be used in multidimensional raster analysis, e.g., trend analysis and multidimensional principal components analysis, the result of which can be further integrated with beekeeping data to assess possible impacts of likely climate change on bees.
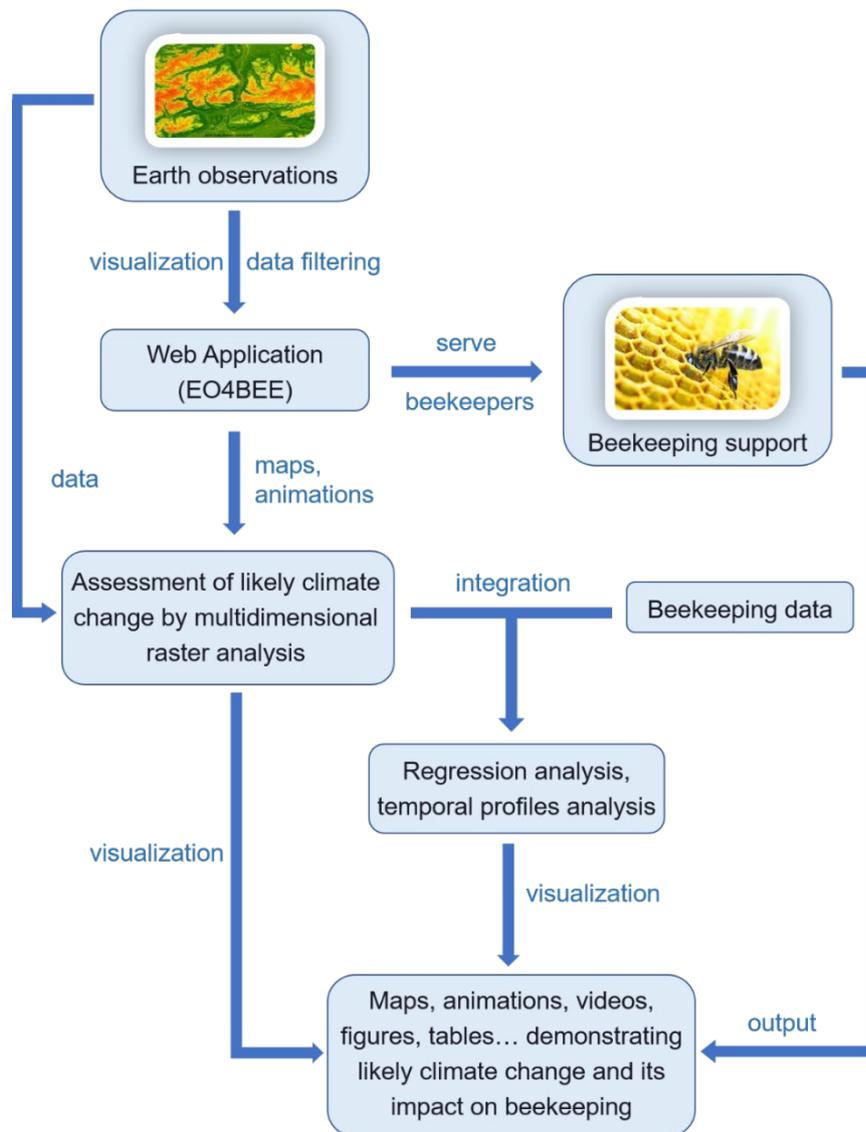

Figure 2 Workflow of the study

3 STATE OF THE ART

This chapter covers the current investigation on the influence of climate conditions on beekeeping, which provides evidence for the most fundamental hypothesis in this paper: climate change could affect the survival of bee colonies. In addition, this section did a comprehensive review of the current research progress on the role that EO data plays in terms of the portrayal of likely climate change impacts on beekeeping.

The study of climate change and the support from EO

Climate change is defined as the long-term variation of climate conditions which is caused mostly by the over emission of greenhouse gas (GHG) from the natural process such as wildfires, earthquakes, volcanic eruptions, etc., and anthropogenic activities including agriculture, industrial production, transportation, etc. (Fawzy et al., 2020). However, it is reported by the Intergovernmental Panel on Climate Change (IPCC) that the rapid rate of modern climate change resulting from activities of human beings is far more significant than the rate of nature-driven climate change and has already led to an approximately one degree Celsius increase of global average temperature compared to the level before (Masson-Delmotte et al., 2018).

The crisis posed by climate change is multifaceted: global warming, large-scale melting of glaciers and snow covers, habitat loss caused by sea-level rise, drastic fluctuation of precipitation, change in wind patterns, extreme weather, etc. (IPCC, 2007). Therefore, it is highly urgent to raise public awareness of the vulnerability of nature in the context of climate change, to closely investigate the mechanism behind these alarming phenomena, and to take effective actions respectively. To achieve these goals, EO plays an indispensable role.

EO is able to provide a large number of planetary-scale datasets of various environmental variables for climate change modeling and simulation, which overcomes the limitation of conventional climate condition measurements and models and thus is fundamental to the scientific advancement of climate change research. The convenience brought by the flexibility of the choice of resolution, sensor, and spatiotemporal scale of satellite images makes remote sensing one of the most efficient ways to understand climate change (Bontemps et al., 2012)

According to a review of the progress of climate change studies based on EO technologies, the potential of EO can be demonstrated in three aspects of the global change study: (1) atmospheric change monitoring based on the detection of air temperature, precipitation, wind, ozone, carbon dioxide, etc., (2) ocean change monitoring based on the detection of sea level, sea surface temperature, water quality, etc., and (3) terrestrial change monitoring based on the observation of land cover, snow cover, glaciers, ground water, etc. (Guo et al., 2014).

Except for providing convenience for monitoring the land, ocean, and atmosphere, EO technologies also contribute a lot to meteorological reanalysis such as the National Center for Environmental Prediction (NCEP) reanalysis (Saha et al., 2010) and the development of mitigation strategies dealing with climate change (Joyce et al., 2009) Furthermore, what cannot be neglected is the role of EO in the education of climate change, for example, Cox et al. (2014) developed tutorials for students to be more informed about and aware of climate change with the support of remote sensing data derived from the NASA satellite products such as Landsat and MODIS.

The prevention of honey bee COlony LOSSes (COLOSS)

Bees play an important role in both the ecologic dynamics of the environment and the economic benefits of agriculture production. However, as early as the mid-2000s, there have been a lot of reports on increasing honey bee colony loss in different regions all around the world (Genersch, 2010).

With the rising concern on bee colony loss, an association named COLOSS (prevention of honey bee COlony LOSSes) was founded in Europe, whose intention is to monitor and understand the pattern of bee colony change and to provide scientific support for the improvement of honey bee well-being (Brodschneider & Gray, 2022). It was originally launched in 2008 and funded by the European Union, focusing primarily on collecting data on bee colony loss in European countries, and was later expanded also to other countries.
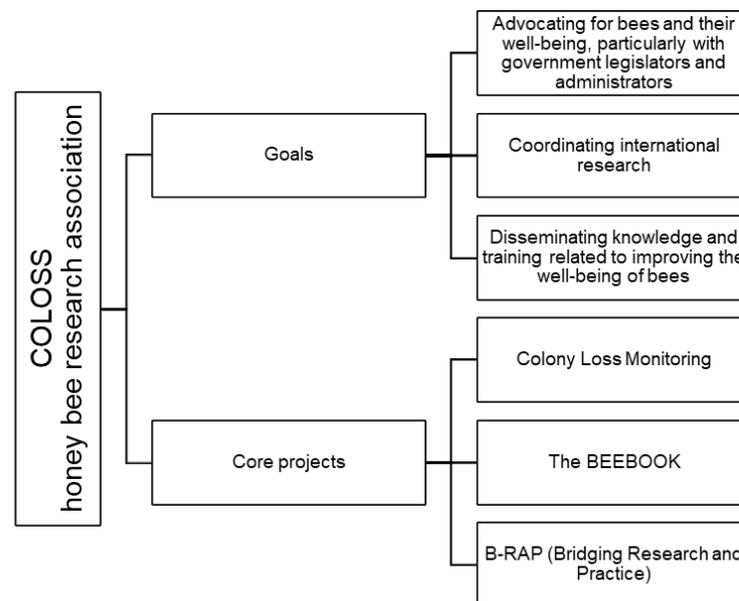
Figure 3 Goals and core projects of COLOSS

The idea of the COLOSS core projects (see Figure 3) is to seek collaboration with local beekeepers and bee enthusiasts by conducting surveys to collect data and calling for data analysis meetings regularly. The great power of COLOSS research lies in the massive amount of bee colony data collected. For instance, in just one year (2018 - 2019), more than 28,000 beekeepers from 35 countries were consulted using standardized questionnaires, with data from more than 738,000 bee colonies acquired, ready for further analysis and diagnosis (Gray et al., 2020).

The output products of the COLOSS projects can be roughly divided into two aspects: theoretical academic products and practical data products for apiculture. Academic output includes open-source articles concentrated on the definitions, approaches, and analysis findings in the study of bee colony loss, published in the COLOSS BEEBOOK or journals like the Journal of Apicultural Research. For example, van der Zee et al. (2013) discussed and examined the approaches of survey design in terms of data collection on bee colony loss. Other output in the forms of data products can be very beneficial to apiculture: statistics can be derived not only to calculate honey bee colony mortality rate (Gray et al., 2020; Brodschneider et al., 2019) but also to identify risk factors related to bee colony loss, such as operation size (Brodschneider et al., 2016, 2018) and forage sources (Gray et al., 2019).

The influence of climate conditions on beekeeping

The survival of bees can be influenced by various factors. Among all the significant challenges for bees like habitat loss, pesticide overuse, invasive species, parasite, disease, etc., climate conditions seem to be one of the most predominant aspects. Weather conditions such as precipitation, temperature, and solar radiation were proven to be related to the in-nest behaviors (Schmickl & Crailsheim, 2007), flight activities (Burrill & Dietz, 1981), thermoregulation (Stabentheiner et al., 2010), and also egg-laying rate (Alhaddad & Darchen, 1995) of honey bees. A national survey on beekeeping taken in the USA revealed that among all the factors, "poor weather" is considered by the beekeepers as the top factor leading to honey bee colony winter loss (Steinhauer et al., 2014).

Although nearly all beekeepers tend to believe that climate has a large impact on bee colonies, turning this intuitive, empirical opinion into scientific fact requires extensive survey records and precise mathematical models. Flores et al. (2019) used the method of precise apiculture (based on a remote hive weight monitoring system) to investigate the hive weight gain of honey bees in Spain (Mediterranean zone with temperate climate conditions) and proved that the drought and high temperature brought about by climate change could hinder the evolution of bee colony and increase the nutrition stress for bees.

The existence of the relation between climate change and bee colony variation can be further confirmed by more research done for different species in different climate zones. The distribution of *E. marianae* in a highly fragmented tropical forest in Brazil is observed to have been affected by precipitation and temperature (Nemésio et al., 2016). Giannini et al. (2012) studied ten different bee species in Brazil using species distribution modeling, and the modeling results indicate that the habitat of nine species (mostly found in the moist forest) will shrink with the progress of future climate change with the exception being only one species named *C. sponsa* whose habitat is mainly located in dry and warm regions. This exception provided evidence for the fact that the impacts of climate change on bees are not necessarily all negative. The distribution of the Australian small carpenter bee species named *C. australensis* is predicted to expand under the situation of global warming and aridification because this bee species has the ability to adapt to aridification and hence has advantages over other species in terms of keeping pace with rapid climate change (Dew et al., 2019).

Although a lot of research such as the ones mentioned above indicates that there is a correlation between climate conditions and the survival of bees, most of these studies are carried out in a natural environment, which makes it difficult to separate the impact of climate conditions on bee colonies from a multitude of other contributing factors such as floral resources, pesticide use, parasites, etc. This limitation was addressed in a study carried out in a botanical garden in Germany (Hofmann et al., 2018). This garden was a very stable environment protected from human intervention, where the floral diversity remained almost the same, and nearly no insecticides were applied. Therefore, the 0.5℃ rise in average temperature from 1997 to 2017 is considered to be the most convincing factor for the fact that the number of warm-preferring bee species increased by 13 while three cold-loving bee species were lost.

In order to fully understand the mechanism of how climate conditions affect the abundance and distribution, what needs to be stressed is that climate conditions can influence bee colonies both directly by altering the behaviors and reproduction of bees and indirectly by affecting the resources that bees are dependent on or predators and parasites of bees.

The direct impact of climate change on the abundance of honey bees was studied in France, and it is observed that climate change can directly alter the behavior, distribution, physiology, and the development of diseases of honey bees (Le Conte & Navajas, 2008). However, there is research showing that the indirect influence climate conditions have on the bees can be more dominant than the direct effect on the bees themselves. Ogilvie et al. (2017) carried out an investigation to examine the relative significance of the direct and indirect effect of climate conditions on the abundance of bumble bees in Colorado, USA. The bee datasets, climate datasets, and flower datasets were combined, modeled, and analyzed, and the result shows that for all the three bee species studied, their abundance was driven more strongly by the indirect effects that temperature and precipitation had on the length of floral days. Apart from this, the indirect effect climate conditions have on the parasites and diseases of bees can also be more noticeable than the direct impact on the bees themselves.

The use of EO in beekeeping

The field of using EO technologies from remote sensing imagery to understand patterns of bee communities and to assist beekeeping still remains under-studied. There are few case studies in this domain, and most of them have only been around since the 2000s.

Galbraith et al. (2015) made a comprehensive review of the current progress, remaining challenges, and the future potential of the use of EO technologies in the study of bees and pollination services. There are numerous EO technologies, including aerial photography, satellite imagery, radar, airborne LiDAR, etc., that can contribute to the understanding of the abundance and distribution of bees. Current approaches employed in the application of remote sensing in bee research can basically be divided into four aspects: landscape characterization, detection of individuals, ecological processes, as well as biodiversity proxies, and species habitat (Galbraith et al., 2015).
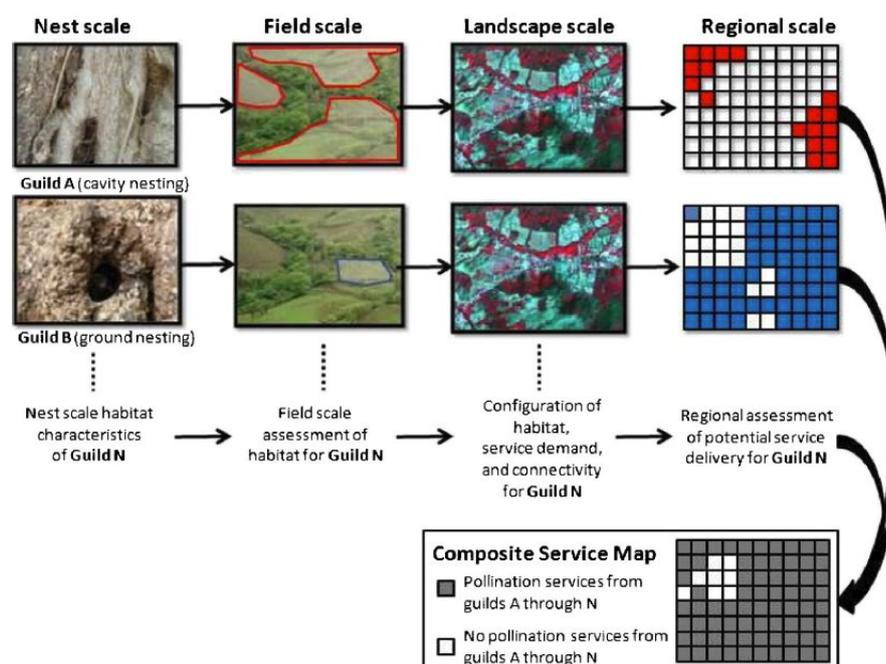

Figure 4 Example of how remote sensing can be used to understand pollination services from bees. The final product, in this case, is a regional map for pollination service provision based on the service demand in the landscape and the habitat availability from guilds A - N.   (Galbraith et al., 2015).

Landscape characterization is one of the most commonly used methodologies in this field, allowing scientists to study the spatial (or even temporal) patterns of the landcover and also the intensity of land use, which is in close relation with the survival and distribution of pollinators like bees. Aerial photography and satellite images can be acquired and analyzed to examine the relationship between the metrics of the bee population and the natural or urbanized environment. For instance, the impacts of forest fragmentation on bee colonies were studied with the assistance of aerial photography and Landsat images in a tropical region (Brosi et al., 2008).

The methods based on the detection of individuals are implemented more often in an indirect way in terms of bee study, e.g., by monitoring the phenology of invasive plants, which can have a large influence on bees (Young et al., 2013; Williams et al., 2011). Detection of the bees themselves by remote sensing is relatively rare due to the fact that they are much smaller in size and also their high agility (Nagendra, 2001). However, it is still possible to use harmonic radar to track the actions of medium-sized bees that are capable of carrying very light tags to observe their flight path and time. One example of the application of this technology is that the existence of the "waggle dance" performed by bees to indicate the location of the floral resource to other bees was verified with the support of harmonic radar (Chapman et al., 2011).

The characteristics of huge spatial extents and especially large time ranges of remote sensing images make it much easier for researchers to study bee-related ecological processes. Nowadays, as multitemporal EO products are becoming more and more easily accessible and also economically more affordable, they can be very constructive in terms of the study of ecological processes related to beekeeping, such as flowering phenology. For instance, a set of satellite imagery in time series can be compared to derive specific information on the blooming and fruiting cycles of a certain plant species (Turner et al., 2003).

Biodiversity proxies such as vegetation index and weather events, which are vital to the survival of bees, can be detected by EO on both spatially and temporally satisfying scales. The use of remote sensing can also improve the habitat suitability model to predict the distribution and movement of a certain species. For example, the distribution map of Africanized Honey Bee (AHB) was improved with a species distribution model using multiple image layers, including MODIS imagery (Jarnevich et al., 2014).

Case studies focused on the application of EO technologies in apiculture are very few, and most of them are carried out in the United States. One of the earliest studies was done in Texas, USA, in 2000. A mathematical algorithm was developed to predict the migration of AHB using earth observations obtained from the advanced very high-resolution radiometer (AVHRR) and other data (Ward & Starks, 2000). The method applied in this case study was to use the normalized difference vegetation index (NDVI) as a metric for biomass to identify areas with similar characteristics as the areas where AHB thrive and then to predict the movement of AHB. The result was quite satisfying, showing a correct prediction rate greater than 60%.

Actually, NASA has contributed a lot to the leading position of the United States the research in this field, with the support of a vast amount of data of its own. A study funded by the NASA Goddard Space Flight Center (GSFC) utilized the vegetation phenology data derived from the MODIS images combined with climate data, bee nectar flow data, and pollen distribution data to disseminate the impacts that climate change and urbanization have on the equilibrium range of AHB and European Honey bee (EHB) in the United

States (Nightingale et al., 2008). The time-related phenology of vegetation was derived from calculated metrics, including NDVI and enhanced vegetation index (EVI), and was analyzed and compared with the honey bee nectar flow (HBNF) data collected from scale hives.

Apart from funding studies like this, GSFC also supported the study of its own scientist Wayne Esias who is at the same time an amateur beekeeper in Maryland and has been collecting weight data of his beehives for more than 15 years since 1992 (Vizcarra, 2010). The trend of earlier spring green-up derived from AVHRR data and the variation of the earlier beginning of the beehive weight gain in spring, i.e., the time when bees start to collect nectar, were found to be approximately synchronized. The reason might be that as the average temperature gets higher because of the climate change, winters become shorter, and also the green-up in springs comes earlier, resulting in an earlier beehive weight gain pattern. This research was later expanded with the support of beehive data from volunteer beekeepers from all over the country, and the same synchronization was confirmed, which can provide important clues for the impacts of climate change on beekeeping.

The theoretical studies mentioned above have provided a solid foundation for the practice of using EO technologies to actually benefit beekeeping. Another research team also from NASA has integrated in-hive data from beekeepers, earth observations from NASA satellites, and data from the U.S. Department of Agriculture (USDA) and used Google Earth Engine (GEE) to build a tool named HIVE-OS to support beekeeping (Rapp et al., 2018). The objectives of the HIVE-OS are to provide a handy tool for the decision-making process of beekeepers, to make it easier for bee scientists to study the correlation between bee health and EO variables, and to contribute to the development of models that can predict events that can threaten the survival of bees in a large scale.

Until now, studies on this topic are still very rare outside the United States. Abou-Shaara (2013) conducted an analysis on land cover change using EO data to uncover the influence of land cover on beekeeping in El-Behera Governorate, Egypt. Landsat images, as well as historical images from google earth, are combined and analyzed in a geographical information system (GIS) to create time-series maps, which can be integrated with beekeeping data to study how land cover change can make a difference to the living situation of bees. Another study in Kenya demonstrated that EO technologies could also benefit apiculture in an indirect way, e.g., by serving as an important auxiliary tool that can be used to improve the prediction map for the distribution of honeybee pests (Makori, 2017). The combination of variables including precipitation and NDVI with the pest data collected from apiaries was applied to improve the accuracy of the honeybee pest ecological niche (EN) models by reducing the overfitting of the EN predicting models.

It can be noticed that the topic of remote sensing application in apiculture in Europe is still somehow under-discussed. Therefore, it is of great significance to focus on the continent of Europe and pave the way for scientists as well as beekeepers and bee enthusiasts in Europe.

Application of GEE in climate change study and visualization

Google Earth Engine (GEE) is a platform that exploits the potential of both remote sensing big data and cloud-computing based on Google's supercomputing competence for geospatial visualization and scientific analysis, hosting a massive archive of publicly available and multi-source satellite imagery for more than 40 years in a data format that is ready for visualization, exploration and spatial analysis (Gorelick et al., 2017). It allows

the users to conduct geospatial visualization and analysis not only on a planetary spatial scale but also for a very long time period, without the cumbersome and extremely time-consuming work of downloading and processing a huge amount of satellite imagery that usually requires a lot of storage space and high-performance computing power. This is of great significance to the more profound and extensive application of remote sensing in multiple domains, as the abundance of EO data continues to grow with the advancement of numerous satellites and sensors with different resolutions of spectrum and space (Amani et al., 2019).

The basic working principles of the GEE can be illustrated in Figure 5. The GEE code editor and customized web apps can utilize functions from the GEE API for JavaScript or Python to send interactive requests or batch queries which are processed by either on-demand computation or batch computation to fetch remote sensing images from the GEE backend data services (Gorelick et al., 2017).
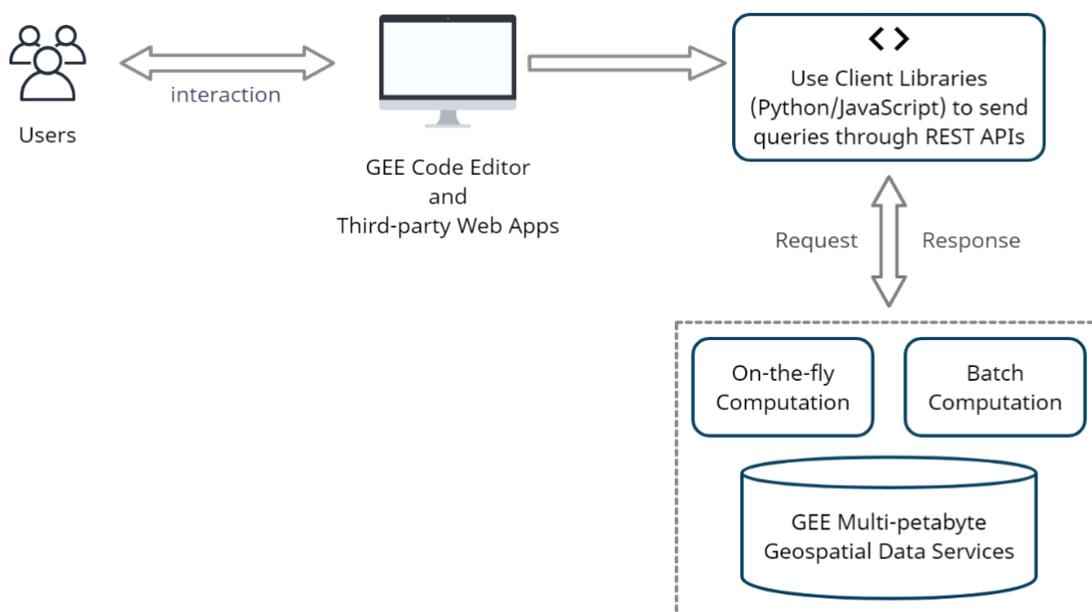
Figure 5 The working principles of GEE

GEE consists of several important features, including the GEE data explorer, built-in algorithms, GEE code editor, and GEE time-lapse, which enables the users to observe, explore and investigate the earth through countless remote sensing datasets in a fast and effortless manner.

The GEE data explorer is an online tool that allows the users to easily browse and search through a huge number of EO datasets as well as other derived datasets available in the near-real-time earth engine data catalog updated frequently on a daily basis with newly acquired images. As shown in Figure 6, the publicly available GEE data archive includes both raw data of satellite imagery and processed datasets, which can generally be divided into four categories: raw imagery data, climate and weather data, geophysical data, and socio-economic data. Among these datasets, the Landsat imagery is likely to be the most often used one by scientific research, with 159 papers using Landsat images, whereas only 80 papers using MODIS from the launch of GEE (2010) to June 2017 (Kumar & Mutanga, 2018). What is worth mentioning is that apart from the existing datasets in the GEE data archive, it is also possible for the users to upload and share personal datasets of their own (Gorelick et al., 2017).
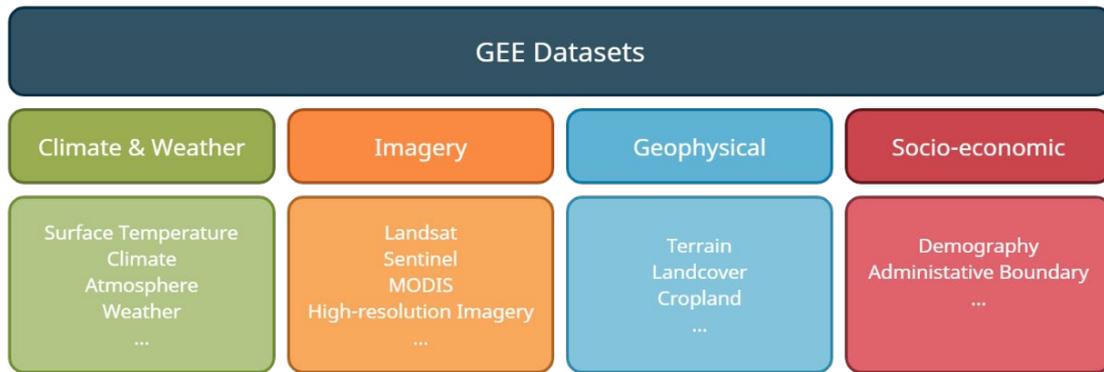
Figure 6 GEE Datasets Categories

The built-in algorithms in the GEE client library designed for the processing and visualization of EO data actually bring the mighty cloud computing power to life. The functions related to image processing (e.g., image classification, band math, convolution, etc.) and geometry operation (e.g., measurements, buffer, intersection, etc.) make GEE not only a public container for a vast amount of earth observations but also a strong geospatial analysis tool for a vast amount of data. For instance, the random forest (RF) classifier, which is a machine-learning-based supervised classification in GEE, was used to realize a more precise local climate zone (LCZ) mapping while harnessing the multi-source nature of GEE images to examine different datasets combinations (Shi & Ling, 2021).
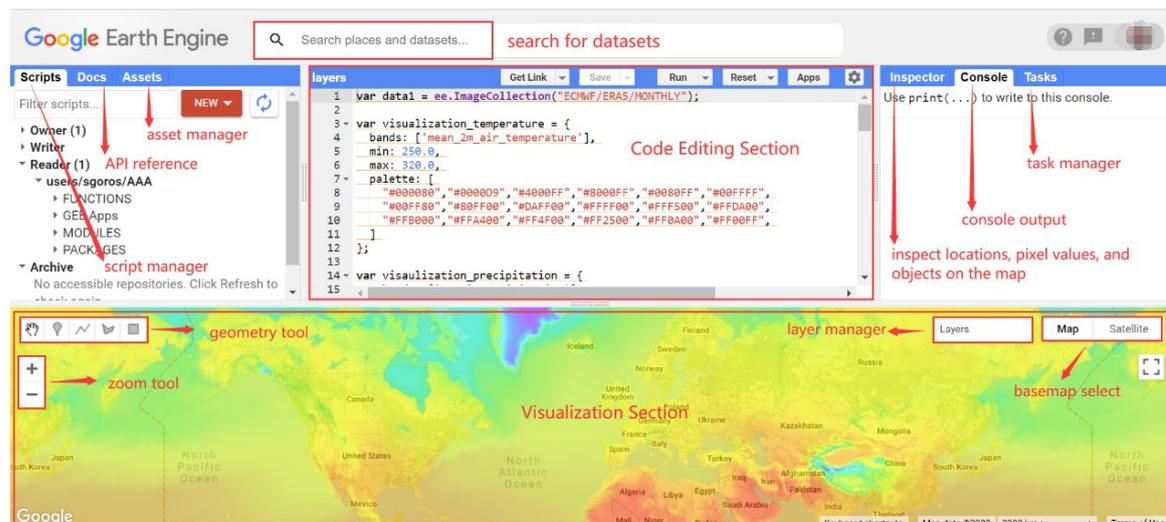
Figure 7 GEE Code Editor

The GEE code editor is an interactive, web-based, and integrated development environment for customized GEE applications and data visualization. As it is displayed in Figure 7, its interface is comprised of several sections:

(1) Dataset search bar;
(2) Main panel for JavaScript code editing and executing;
(3) Document management section for management of script, API reference, and assets;
(4) Console output and task manager section, including a pixel/object inspector;
(5) Visualization result and application preview section with several basic map controls.

These five sections together allow scientists, developers, as well as enthusiasts to visualize, analyze and even quantify various characteristics of the earth's surface by

simply inserting a snippet of JavaScript code without wasting time on downloading a large amount of different imagery data.

The GEE time-lapse is a relatively new feature developed by Google, which is considered to be the most significant technical update of the Google Earth platform since 2017, and more than 24 million remote-sensed images from nearly forty years have been used to compile the interactive time-lapse videos of the whole planet (Chanthadavong, 2021). This makes the investigation of where and when the earth's surface has changed on a large spatiotemporal scale unprecedentedly convenient and intuitive.

The application of GEE can benefit many domains, including vegetation analysis, agriculture management, climate change, urban study, disaster monitoring, land cover investigation, hydrology research, etc. (Amani, 2020). According to the special issue focusing on a summary of research application of GEE published by the journal "Remote Sensing of Environment", only five out of 239 studies harnessing GEE are concentrated on climate change until April 2018 (Wang, 2020). Hence the importance and urgency of deeper exploitation of the potential of GEE from the perspective of climate change study.

The technical nature of GEE discussed previously makes it the perfect assistance tool for research on climate change as well as global climate monitoring. Bunting et al. (2019) took advantage of the strong computing power and abundance of EO datasets of GEE and managed to quantify the ecological response of plants to climate change in southwestern America. The emergence of a global climate monitoring web app with good availability of time span named "Climate Engine" developed by Huntington et al. (2017) was great progress in climate study and visualization. It offers an opportunity for people to visualize, observe, summarize and interpret the evolution of climate variables such as air temperature and precipitation in a revolutionary and interactive way with small limitations of the scale of both space and time. Powered by GEE, Climate Engine offers a highly customizable user interface (Figure 8), making the on-demand visualization and analysis of numerous variables of climate conditions fast and effortless. It is also possible to make a time-series plot of the chosen variable at a certain point or region, which is a great reference for the implementation of the web app that this paper aims to achieve.
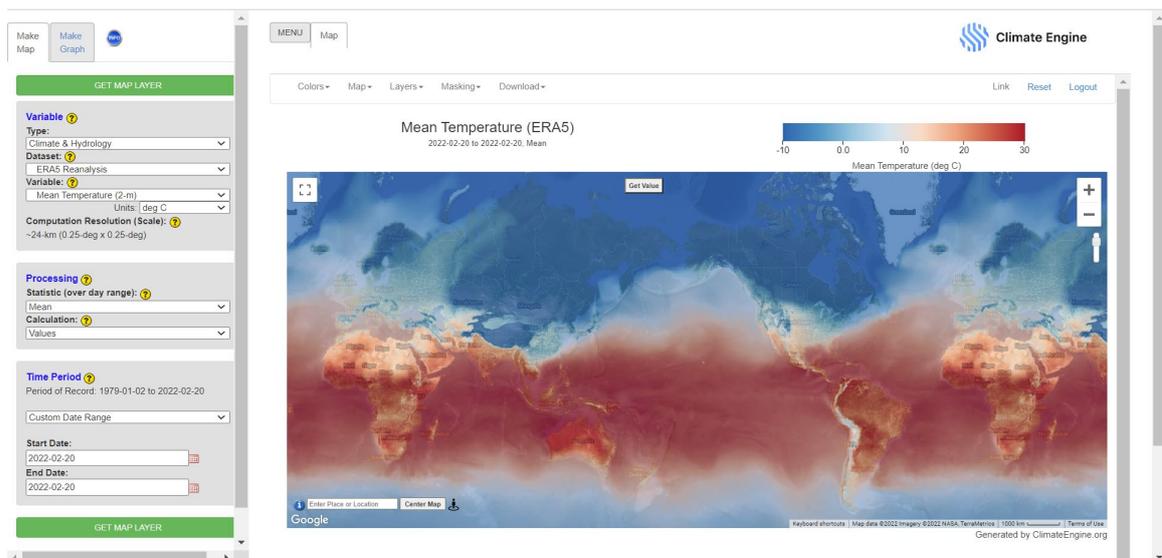

Figure 8 Interface of Climate Engine

4 DEVELOPMENT OF THE WEB APPLICATION

The procedure of the development of the web application for beekeeping support in Europe utilizing GEE earth observation data can be divided into four stages: determining the goals that this web app is about to achieve, designing the user interface and user interaction, implementing core functions, testing, and publishing of the web app.

4.1 Objectives of the web app

The final goal of this web application is to take advantage of the big repository of EO data and the remarkable cloud computing power of GEE to visualize the change in climate conditions that are vital to the survival of bees in a broad time span and at a large scale. It serves to provide a handy tool for beekeepers, bee experts, and bee enthusiasts in Europe to investigate the evolution of climate conditions as well as other EO variables relevant to the living environment of bees so as to study possible impacts of likely climate change on beekeeping.

To achieve the goal stated above, the web app, which was named "EO4BEE", must fulfill the following objectives:

(1) allow EO4BEE users to select and visualize different EO variables that are related to beekeeping, such as temperature and precipitation;

(2) allow EO4BEE users to browse through a time series of any time span within the time availability of the data source of relevant variables to see the overall changes;

(3) allow EO4BEE users to inspect the exact value of their variable of interest at a specific location and a specific time;

(4) allow EO4BEE users to plot the change of a certain variable over time at a specific location;

(5) allow EO4BEE users to generate and download customized timelapse gifs of their variable of interest at any scale within Europe.

4.2 Data filtering

There are a large number of datasets accessible through GEE, and they need to be filtered to fit the objectives of the EO4BEE web app. The variables chosen for the web app are listed in Table 2. Details about the data source of these variables, including data provider and time availability, can be found in the table in attachment 1.

Temperature and precipitation are both important bioclimate variables to evaluate the extent of climate change. The reason why there are two sources for temperature and precipitation is that they have different resolution and time availability, which means both options can provide valuable information for the user from a different perspective.

NDVI, land cover, and soil moisture are included because these variables are closely related to the habitat and food resources (mostly floral resources) of the bees. Sulphur dioxide and PM2.5 are also selected for this web app because they can be good indicators of air pollution, which can not only affect bee health directly (Hillmann, 1972) but also influence the survival of bees indirectly by affecting the flowering process (McFrederick et al., 2008).

Table 2 Earth observation variable chosen for the EO4BEE web app

Variable	Description	Resolution	Data source
Temperature	Average daytime land surface temperature (˚C*)	1000 m	MOD11A1.006
Precipitation	Precipitation accumulation (mm)	4638.3 m	TerraClimate
Temperature (ERA5)	Average air temperature at 2m height (K)	27830 m	ERA5 Monthly Aggregates
Precipitation (ERA5)	Total precipitation (m)	27830 m	ERA5 Monthly Aggregates
NDVI	Normalized Difference Vegetation Index	30 m	Landsat 7 Collection 1
Landcover	Land cover	100 m	Copernicus CORINE Land Cover
Soil moisture	Soil moisture at 0 - 10 cm underground (m^3 /m^3)	11132 m	FLDAS
Sulphur dioxide	SO2 vertical column density at ground level, calculated using the DOAS technique (mol/m^2)	1113.2 m	Sentinel-5P NRTI SO2
PM2.5	Particulate matter d < 2.5 um (kg/ m^3)	44528 m	Copernicus Atmosphere Monitoring Service

*: The unit of the original data is K with a scale of 0.02 and is converted to ℃ in the web app.

**: FLDAS: Famine early warning systems network Land Data Assimilation System

4.3 User interface and interaction design

The web app was developed in a single-page app manner. All the fundamental interactions are expected to be done on the same web page except for some hyperlinks to relevant resources.

4.3.1 User interface design

According to the objectives that the web app is supposed to achieve, the user interface can be divided into three sections: user guidelines, time-series visualization, and a timelapse generator. Prototypes are made for each section respectively to guide the process of web application development.

User guidelines

The user guidelines section is designed as a static section without interaction, merely serving the purpose of information display. The prototype of this section is shown in Figure 9. It serves the following purposes:

(1) giving a brief introduction on the aims of this web app;
(2) showing the EO4BEE users how to interact with the app to get their desired result in detailed steps;
(3) displaying supplementary information about the author, the open-source code repository, and the data source used for the web application.
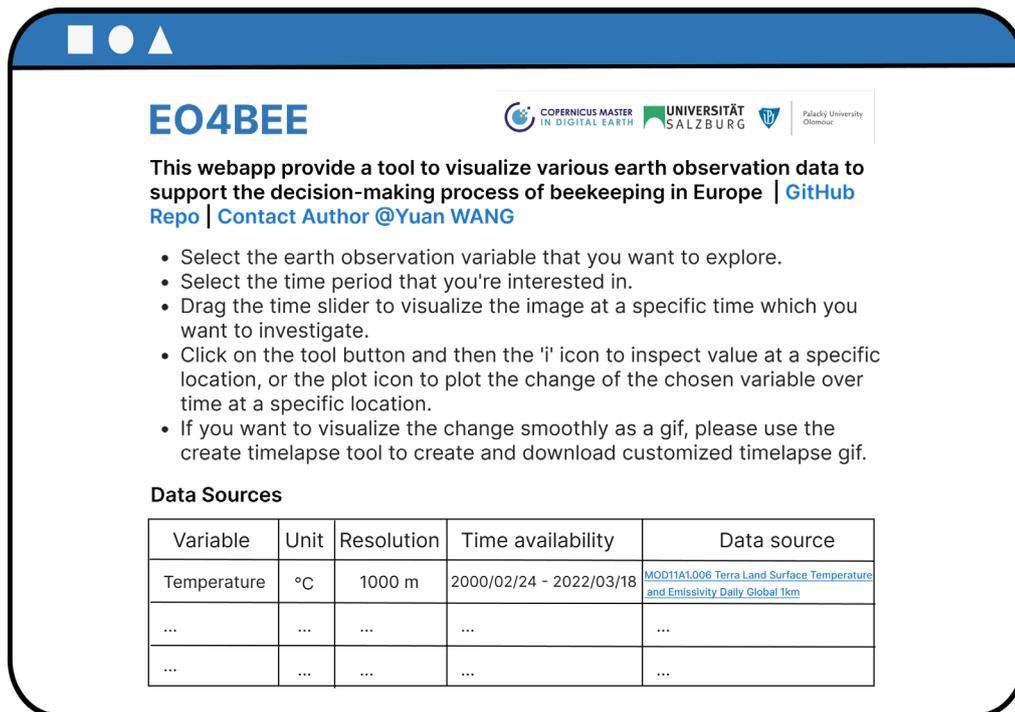
Figure 9 Prototype for user guidelines section

Time series visualization

The time series visualization section consists of 2 parts: user input and visualization output. The user input part is comprised of several dropdown widgets which allow users to select the layer of interest, the year of start, and the year of the end, respectively, as well as a button to execute the action of visualization. The visualization output part should be a map window showing the result of the custom user query, with several map control buttons (home button, zoom button, and tool button) and a time slider widget to interact with the image time series.

Figure 10 Prototype for the time series visualization section

Timelapse generator

The timelapse generator section is also comprised of two parts: user input and timelapse output.

The user input part includes multiple input widgets to define the parameters to create a customized timelapse: a dropdown menu to select the dataset of interest (temperature, precipitation, NDVI, etc.), a text input box to type in the title of the timelapse, two date picker to choose the start date and end date, an integer slider to define the number of frames per second, a check box to decide whether to add the progress bar to the timelapse, a color picker to determine the color of the progress bar, an integer slider to decide the size of the font, another color picker to choose the color of the font, a dropdown menu the select the frequency at which the timelapse would be created, and finally, a button to execute the action of generation of the timelapse.

The output part is the map window in which the timelapse is created based on the dataset selected, and the custom parameters entered by the user will be displayed at the corresponding position.
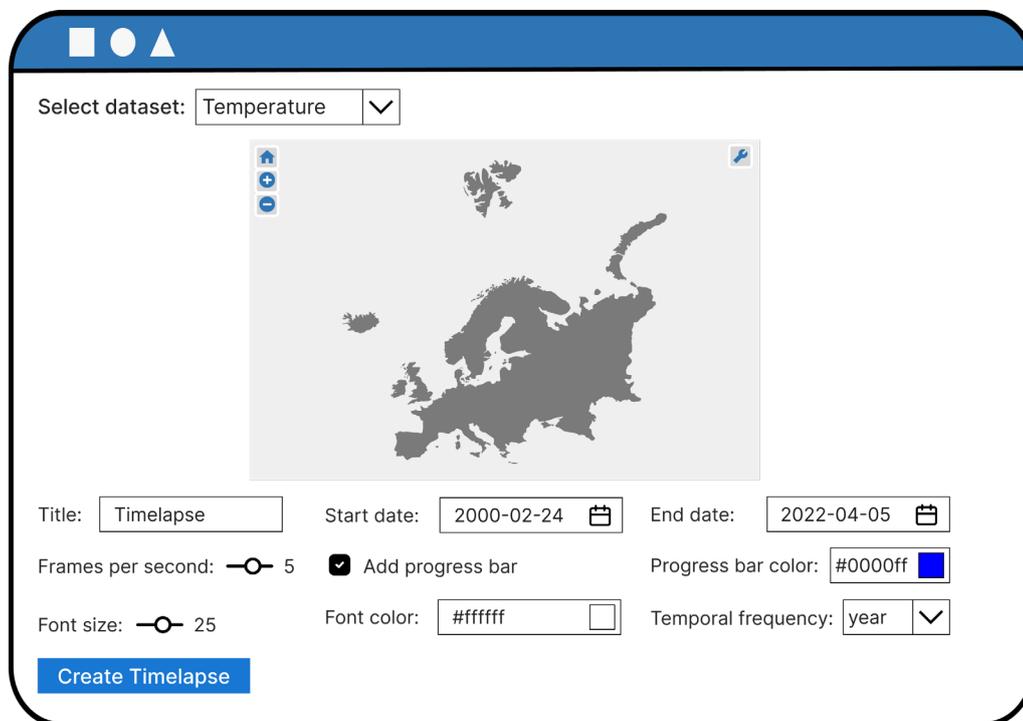
Figure 11 Prototype for the timelapse generator section

4.3.2 User interaction design

The user interaction design will be elaborated accordingly for the three sections of the user interface stated above.

User guidelines interaction design

The interaction design of the user guidelines section is not related to any core function of this web application and only involves some click event of several hyperlinks. As shown in the user interface prototype in Figure 9, The text colored in blue should be linked to the corresponding web resource. When the user clicks on "GitHub Repo" or the name of the data source, the webpage is supposed to jump to the GitHub repository of the source code or the detailed information page of the clicked dataset, respectively. What is slightly

different is the click event of "contact author", which is expected to open a new window to send an email to the author's email address when triggered.

Time series visualization interaction design

Firstly, the user selects a layer of interest from the available layer list (Table 3). After the layer is determined, the list of values in the dropdown menu for the start year and end year will be updated according to the time availability of the data source that the chosen layer is derived from (see attachment 1 and Table 2). What is worth mentioning is that if the frequency of time series related to the chosen layer is "per month", two new dropdown menus will emerge to allow the user to select also the "start month" and "end month". Based on these selections, the corresponding query of the image time series will be performed when the "visualize" button is clicked. If the user did not make any previous selection, default values are applied to the visualization.

Table 3 Available layer list

Available layers	Frequency of time series
Annual average temperature	Per year
Monthly average temperature	Per month
Annual total precipitation	Per year
Monthly total precipitation	Per month
NDVI	Per year
Landcover	One image each from 1989-1998, 1999-2001, 2005-2007, 2011-2012, 2017-2018
Soil moisture (yearly mean)	Per year
Soil moisture (monthly mean)	Per month
PM 2.5 (yearly mean)	Per year
PM 2.5 (monthly mean)	Per month
Sulphur Dioxide (yearly mean)	Per year
Sulphur Dioxide (monthly mean)	Per month

It takes a few seconds (sometimes longer, depending on the amount of data queried) for the expected visualization output, which is ready for further interaction to appear in the map window. Users can drag the control on the time slider to display the image at a specific year (or month), play or pause continuous autoplay of the time series, and go to the preceding or the following image by interacting with the time controller.
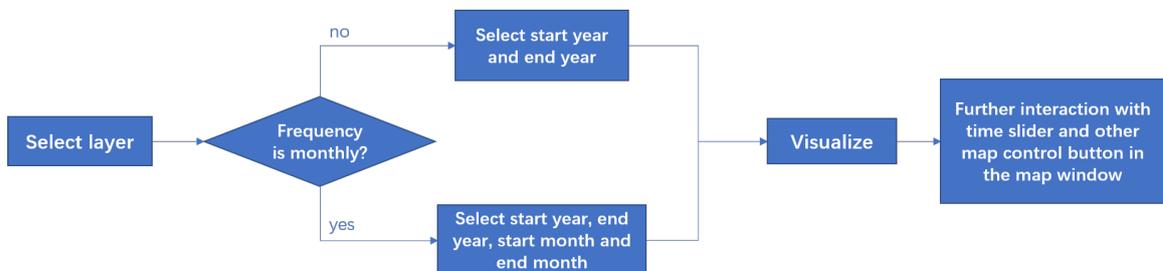

Figure 12 Time series visualization interaction design

Additionally, the tool button on the upper right corner of the map window offers a variety of ways to interact with the visualization result when clicked, e.g., switching on and off

certain layers, inspecting the exact value at a specific location, and creating a line chart showing the change of the chosen variable over time when users click at a certain location on the map. The interaction design of this section is illustrated in Figure 12.

Timelapse generator interaction design

The interaction design of the timelapse generator is similar to the one of time series visualization. Above all, the user selects the dataset of interest from the list of datasets (Table 4) in the dropdown menu.

Table 4 List of datasets for timelapse

Dataset	Available temporal frequency
Temperature	year, month
Precipitation	year, month
Temperature (ERA5)	year, month
Precipitation (ERA5)	year, month
NDVI	year, month
Landcover	year
Soil moisture	year, month
PM 2.5	year, month, day
Sulphur Dioxide	year, month, day

After the dataset is picked, the input form of parameters for timelapse generation will be automatically updated: the default start date and end date are changed to match the time availability extent of the relevant data source, and the options in the temporal frequency dropdown menu are also updated according to the available ones of the chosen dataset. Before creating the timelapse, users are also supposed to draw a feature using the geometry tool on the map to specify the spatial extent in which the timelapse will be generated.
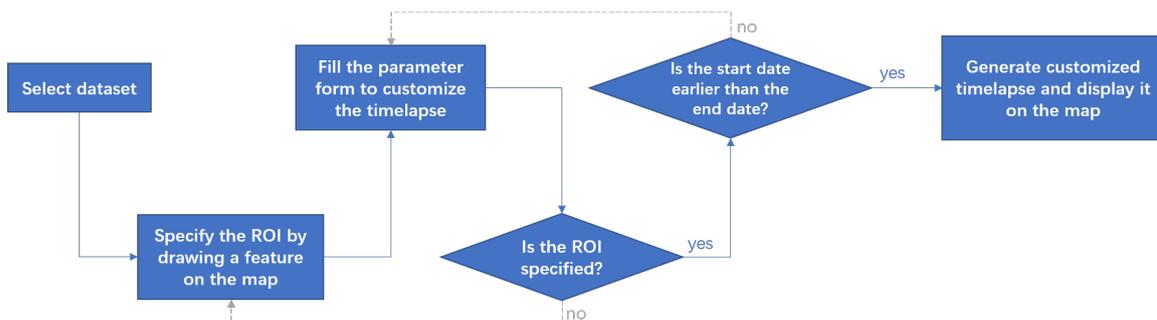
Figure 13 Timelapse generator interaction design

When the click event of the "create timelapse" button is triggered, the web app will firstly go through two conditional judgments: 1) determining whether the start date is earlier than the end date; if not, ask the user to refill the value, 2) determining if the region of interest (ROI) is specified or not, if not, ask the user to draw a feature on the map. Only if these two conditions are satisfied the customized timelapse will be generated and visualized based on the ROI and parameters form specified by users. Users are able to download the gif to their local computer by right-clicking on the timelapse. If the user did not pick or fill any input values, default values are applied to the parameter form, but

users still have to specify an ROI since no default extent was predefined for this function. The whole interaction design of this section is depicted in Figure 13.

4.4 Function implementing

4.4.1 Development environment setup

The development of the EO4BEE web application requires the installation of Anaconda and specific environment settings. After starting the Anaconda Prompt, the following steps are executed to setup the necessary environment:

(1) Create a new Conda environment with Python for the development of EO4BEE:

```
$ conda create -n geebee python=3.8
```

(2) Activate the environment created in the last step:

```
$ conda activate geebee
```

(3) Install the geemap Python package, which is essential for the development of all the core functions in the web app:

```
$ pip install geemap
```

(4) Install Jupyter Notebook extensions for a better development interface in Jupyter Notebook:

```
$ conda install jupyter_contrib_nbextensions -c conda-forge
$ jupyter contrib nbextension install –user
```

Additionally, the authentication of the google earth engine is required for the functioning of the geemap Python package. The presupposition is that a google earth engine account is already created. In the Anaconda terminal, use the command "$ python" to enter the Python interactive shell and then use the Python statements below to authenticate the google earth engine:

```
>>> import ee
>>> ee.Authenticate()
```

These two Python statements will start the browser and open the login page of the google earth engine. Once the credentials for login have been verified, an authorization code will be generated, which can be pasted back into the terminal to complete the authentication procedure. a GEE authorization token will be stored in a configuration file under the path stated below:

```
C:\\Users\\USERNAME\\.config\\earthengine\\credentials
```

The token is stored in this file in the format below and will be used when the web map is deployed to the server.

```
{"refresh_token:" earth_engine_token}
```

The last step is to start Jupyter Notebook, create a new file, and import all the libraries required for the development of this web app:

```
import ee
import geemap
import ipywidgets as widgets
from datetime import datetime
from IPython.display import Image
import copy
```

4.4.2 Time series visualization

Widgets implementing

First of all, the default style of all the widgets should be defined:

```
style = {'description_width': 'initial'}
layout_small = widgets.Layout(width='180px')
```

Then all the user input widgets are initialized. The layer selecting dropdown menu is defined directly with the available layers listed in Table 3; however, the time span selector is defined in an interactive way since the widgets for start year, end year, start month, and end month have to be updated to match the value of the selected layer according to the user interaction design.

```
layer = widgets.Dropdown(
  description='Select Layer:',
  options = ['Annual Average Temperature', 'Monthly Average
             Temperature', 'Annual Total Precipitation', 'Monthly
             Total Precipitation', 'NDVI', 'Landcover', 'Soil
             Moisture (yearly mean)','Soil Moisture (monthly mean)',
             'PM2.5 (yearly mean)', 'PM2.5 (monthly mean)', 'Sulphur
             Dioxide (yearly mean)','Sulphur Dioxide (monthly
             mean)'],
  value='Annual Average Temperature',
  style=style)
time_selector = widgets.Output()
```

The output widget "time_selector" will be updated to display the right type (with or without month selector) of time span widgets with the related default value when change is observed on the "layer" widget:

```
# Callback function for the change of the layer selector's value
def on_layer_change(change):
    time_selector.clear_output()
    layer = change['new']
    getYearSelector(layer)
# When the layer is changed, change the range of the year selector
layer.observe(on_layer_change, names='value')
```

The function " getYearSelector" is responsible for displaying the corresponding time span selection widgets in the "time_selector" output widget according the incoming "layer" parameter. Below is a simplified code snippet showing only the important part, complete codes can be found in the attachment "eo4bee.ipynb".

```
def getYearSelector(layer):
    time_selector.clear_output()
    timespan = getAvailableYears(layer)
    global start_year = widgets.Dropdown( description='Start year:',
        options= timespan, value=timespan[0])
    global end_year = widgets.Dropdown( description='End year:',
        options= timespan, value=timespan[len(timespan)-1])
    if layer in layers_monthly:
        with time_selector:
```

```
                   display(widgets.HBox([start_year,start_month,
                                   end_year,end_month]))
               return
       with time_selector:
               display(widgets.HBox([start_year, end_year]))
```

Lastly, the button widget to visualize the time series is defined:

```
show_layer = widgets.Button(
    description='Visualize',
    button_style='primary',
    tooltip='Click to visualize the selected layer',
    style=style,)
```

Time series visualization implementing

The output images of the queried time series should be displayed in the map window, which is initialized to be centered in Europe:

```
Map = geemap.Map()
Map.set_center(14, 52, 4)
```

The core functionality of this section is done by the "showLayer" method, which is supposed to be evoked when users click on the "visualize" button. According to the user input parameters, including the selected layer, start time, and end time, the required time-series images will be queried from GEE and added to the map window. The following code snippet that is simplified shows how this method is implemented.

```
def showLayer():
    if layer.value in layers_monthly:
        start_date = start_year.value + '-'+ start_month.value + '-01'
        end_date = end_year.value + '-'+ end_month.value + '-' +
                     end_day_list[end_month.value]
    else:
        start_date = start_year.value + '-01-01'
        end_date = end_year.value + '-12-31'
    if layer.value == 'Annual Average Temperature':
        collection = ee.ImageCollection('MODIS/006/MOD11A1')
            .select('LST_Day_1km').filterDate(start_date,end_date)
        collection_celsius = collection.map(toCelsius)
        collection_yearly_mean = geemap.create_timeseries(
            collection_celsius, start_date, end_date,
            frequency='year', reducer='mean')
        vis_params = {
            'min': -5,
            'max': 30,
            'opacity': 0.7,
            'palette': temperature_pallette}
        Map.add_time_slider(collection_yearly_mean, vis_params, '',
            'Time series of annual average air temperature(℃) at 2m',
            time_interval=2)
    if layer.value == 'Monthly Average Temperature':
        …

if layer.value == …
```

Firstly, it assigns values to the start date and end date in the required date format "yyyy-mm-dd" depending on whether the chosen layer is with monthly frequency. Then, according to the value of the selected layer, the "if" condition decides which image collection to query from GEE, as well as in what time span and at which frequency to create the time series. In the simplified code snippet above, the codes to display image time series and add the time slider control for only one layer are shown to avoid repetition since the code structure remains the same for all of the layers, with the variations being: the image collection code, the band name, the frequency, the reducer, and the visualization parameters, and they are all listed in the table in attachment 2. Complete codes are available in the attachment "eo4bee.ipynb".

Finally, to realize the functionality of the "visualize" button, the method to create the image time series needs to be linked to the click event of the button:

```
# function to be executed when the visualize button is clicked
def vis_clicked(b):
    if hasattr(Map,'slider_ctrl'):
        # evoke the click event of the close button of the time slider
        Map.slider_ctrl.widget.children[4].click()
    showLayer()
# watch the click event of the visualize button
show_layer.on_click(vis_clicked)
```

A detail worth mentioning is that before showing the queried image time series on the map and adding the time slider control, the previous layer and time slider control has to be removed to avoid multiple time slider controls which could be confusing to users.

4.4.3 Timelapse generation

Widgets implementing

In accordance with the user interface design, the following user input widgets are implemented.

(1) Dataset selection dropdown widget:

```
dataset = widgets.Dropdown(
    description = 'Select Dataset:',
    options = ['Temperature', 'Precipitation', 'Temperature (ERA5)',
        'Precipitation (ERA5)','NDVI', 'Landcover', 'Soil Moisture',
        'PM2.5','Sulphur Dioxide'],
    value = 'Temperature')
```

(2) Text input widget for the title of the timelapse:

```
title = widgets.Text( value = 'Timelapse', placeholder = 'Enter title
    for the timelapse', description = 'Title:')
```

(3) The date picker widgets for start date and end date, the default value of which is supposed to be set to the extent of the time availability of the chosen dataset and should be updated accordingly when the value of the chosen dataset selector is changed:

```
start_date = widgets.DatePicker(
  description='Start date:',
  value=datetime.strptime(TimeSpanList[dataset.value][0], '%Y-%m-%d'))
```

```
end_date = widgets.DatePicker(
  description='End date:',
  value=datetime.strptime(TimeSpanList[dataset.value][1],'%Y-%m-%d'))
```

(4) Integer slider widget to specify the play speed of the timelapse:

```
speed = widgets.IntSlider(value=5, min=1, max=30, step=1, description=
        'Frames per second:', orientation='horizontal')
```

(5) Check box widget to indicate whether to add the progress bar or not and color picker to specify the color of the progress bar:

```
add_progress_bar = widgets.Checkbox(value = True, description = 'Add
        progress bar', disabled = False, indent = False)
progress_bar_color = widgets.ColorPicker(concise=False, description=
        'Progress bar color:', value='#0000ff', disabled=False)
```

(6) Integer slider to specify the font size of the text on the timelapse and another color picker to choose the font color of the text:

```
font_size = widgets.IntSlider(value=25, min=10, max=50, step=1,
        description= 'Font size:', orientation='horizontal')
font_color = widgets.ColorPicker(concise=False, description='Font
        color:', value='#ffffff', disabled=False)
```

(7) Dropdown box to choose the temporal frequency in which the timelapse is generated:

```
frequency  =  widgets.Dropdown(options=FrequencyList[dataset.value],
value='year', description='Temporal frequency:', disabled=False)
```

(8) Submit button whose click event is linked to the method of creating the timelapse using the specified parameters:

```
submit = widgets.Button(description='Create Timelapse', button_style=
        'primary', tooltip='Click to create timelapse')
submit.on_click(submit_clicked)
```

According the interaction design, the default values of the start date, end date and frequency widgets have to be automatically updated when the value of the chosen dataset is changed:

```
def on_dataset_change(change):
  dataset = change['new']
  start_date.value=datetime.strptime(TimeSpanList[dataset][0],'%Y-%m-%d')
  end_date.value=datetime.strptime(TimeSpanList[dataset][1],'%Y-%m-%d')
  frequency.options = FrequencyList[dataset]
  dataset.observe(on_dataset_change, names='value')
```

Timelapse generation implementing

The core functionality of this section is completed by the method "submit_clicked", the implementation of which is programmed fully in accordance with the user interaction design. Firstly, the values of the start date and end date are compared. If the end date is earlier than the start date, the function will stop proceeding and warn users about the error and ask them to refill the values:

```
if start_date.value >= end_date.value:
    print('The end date must be later than the start date.')
    return
```

Then the program continues to check if the geometry to specify the spatial extent is drawn by the user; if not, stop proceeding and ask users to draw a feature on the map:

```
feature = Map1.draw_last_feature
if feature is None:
    print('Please draw a feature on the map to specify the ROI')
    return
```

After these two conditions are met, the program assigns the output file directory of the timelapse gif and makes a deep copy of the visualization parameters, the data range of which is changed for temperature and precipitation datasets when the frequency is "year" to ensure the best visualization color. The reason why it must be a deep copy is that the modification of the visualization parameter will also be applied to the original visualization parameter list if it is with only a shallow copy. The simplified code snippet shows how it was implemented.

```
out_gif = geemap.temp_file_path(".gif")
VisParams = copy.deepcopy(VisParamList[dataset.value])
if dataset.value == 'Precipitation' and frequency.value == 'year':
    VisParams['min'] = 0.4
    VisParams['max'] = 2.0
if dataset.value == Temperature and frequency.value == 'year':
    …
```

The generation of timelapse is realized by the method " create_timelapse" from the geemap module, which create and display the timelapse customized by all the parameters defined previously.

```
try:
  out_gif = geemap.create_timelapse(
    collection=ImgCollList[dataset.value],
    start_date = start_date.value.strftime("%Y-%m-%d"),
    end_date = end_date.value.strftime("%Y-%m-%d"),
    region = roi, frequency = frequency.value,
    reducer = ReducerList[dataset.value],
    date_format = 'YYYY-MM-dd', out_gif=out_gif,
    bands = BandList[dataset.value],
    palette = PaletteList[dataset.value], vis_params = VisParams,
    dimensions = 768, frames_per_second = speed.value,
    crs = "EPSG:3857", title = title.value, title_xy = ("2%", "90%"),
    add_text = True, text_xy = ("2%", "2%"), text_sequence = None,
    font_size = font_size.value, font_color = font_color.value,
    add_progress_bar = add_progress_bar.value,
    progress_bar_color = progress_bar_color.value,
    progress_bar_height = 5, loop = 0)
  geojson = geemap.ee_to_geojson(roi)
  bounds = geemap.minimum_bounding_box(geojson)
  layer_name = 'timelapse'
  Map1.image_overlay(url=out_gif, bounds=bounds, name=layer_name)
  print('Right click to save the image to your local computer.')
  display(Image(data=open(out_gif, 'rb').read(), format='gif'))
except:
  empty_text.error("An error occurred while computing the timelapse. You
  probably requested too much data. Try reducing the ROI or timespan.")
```

4.5 Testing and publishing

4.5.1 Testing and refinement

Testing of core functions

The purpose of testing is to ensure the implementation quality of the web application and to confirm that the web app is able to accomplish the objectives in an expected way. The main tasks of testing include identifying runtime errors, examining the effectiveness of the assembly process from a low level to a high level of the application components, and verifying whether the application meets the user interface and interaction design specified previously in the documentation. Testing can not only validate the quality of the application but also provide developers with information for the assessment of potential risk.

There are various types of testing approaches, e.g., static testing and dynamic testing, which are differentiated based on the execution state during testing. The static testing is done without running the application. It relies on analyzing the statements, structures, and procedures of the source code to check whether future execution of the application would throw errors. Common errors could be undefined or repeatedly defined variables, misspellings of predefined methods, mismatched parameters, etc. On the other hand, dynamic testing is carried out when the application is actually running. It compares the acquired results with the expected results and analyzes the efficiency and robustness of the program, which can basically break into three steps: construction of testing instances, simulation of interactions, and evaluation of the results. For the "EO4BEE" web application in this study, static testing is already interspersed with the process of implementation. Hence only dynamic testing will be elaborated in this section.

According to the user interface and interaction design, every single step in Figure 12 and Figure 13 is tested with instances one by one:

(1) Change the value of the layer selector dropdown menu to test if the time span selection widgets update accordingly by comparing the updated default values from the web app with the extent of time availability of relevant data sources listed in the table in attachment 1. The screen shots in Figure 14 are results from testing instances showing how the app reacts when the user changes the value of the selected layer from "Annual Average Temperature" to "Monthly Total Precipitation". The default values of time span selection widgets for all the layers have been tested and verified one after the other in comparison with the expected time availabilities.

Figure 14 Updates of time span selection widgets for annual average temperature (a) and monthly total precipitation (b)

(2) Go through all the layers with the default time span to test if the image time series can be queried and displayed correctly. If yes, test all the layers again with a random

time span to see if the application throws any errors. Furthermore, test if the slider, the play button, the pause button, and the close button in the time series control can function as expected. The screenshot in Figure 15 is a testing example that shows the visualization results of the query for the NDVI time series from 1999 to 2021.
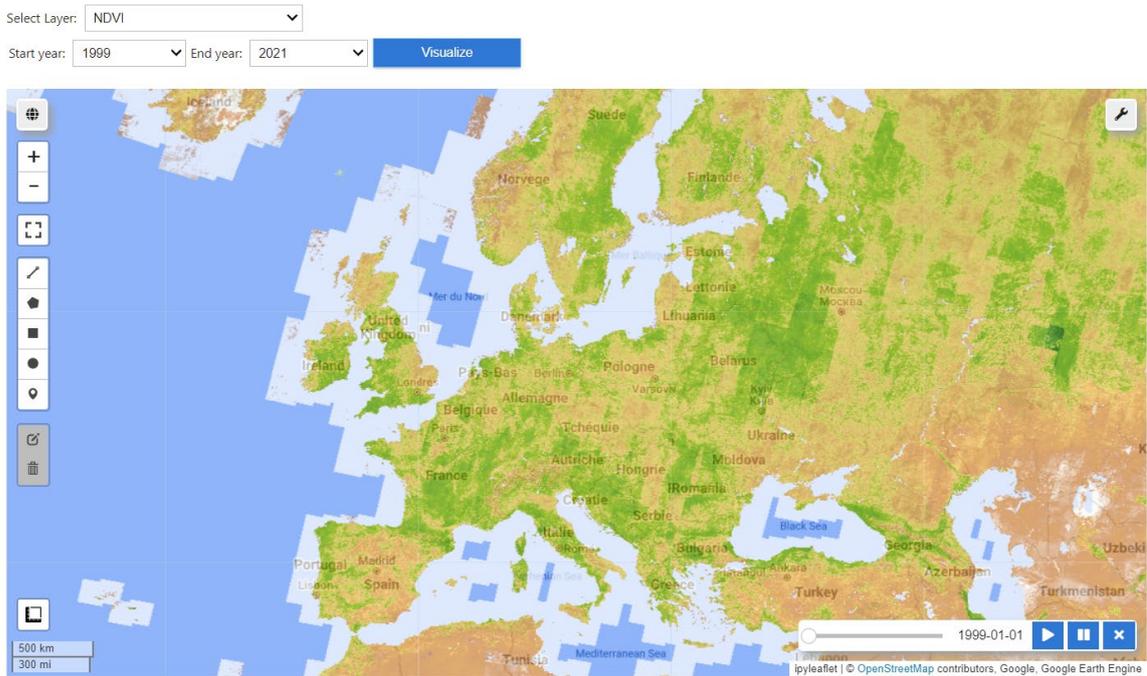

Figure 15 Query results of NDVI time series from 1999 to 2021

(3) Check if the tools in the toolbox at the top right corner of the map window can work properly. Among all these tools, the most important ones are the inspector and the plotting tool, which should be examined with extra care.
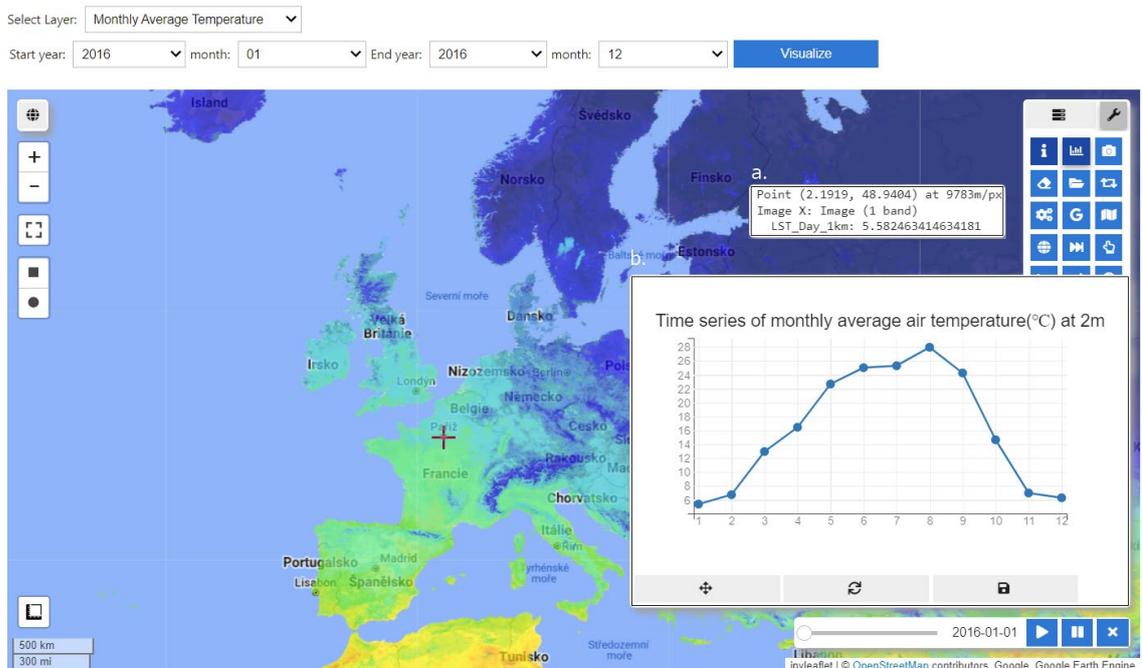
Figure 16 Testing of inspector tool (a) and plotting tool (b)

The testing examples in Figure 16 are done with the instance "monthly average temperature from January 2016 to December 2016", with the inspector tool showing the monthly average temperature in January 2016 and the plotting tool showing the change of monthly average temperature for the whole year of 2016 at the specified location.

(4) Change the value of the dataset selector in the timelapse generator section to test if the date picker widgets for start date and end date refresh accordingly by comparing the updated defaults dates from the web app with the time availability of the source of the selected dataset. The screenshots in Figure 17 are results from testing instances showing how the web application responds to the change of the selected dataset from "Temperature" to "Precipitation". The default values of date picker widgets for all of the datasets listed in Table 4 have been tested and compared with the expected time availabilities in attachment 1 on an individual basis.

Figure 17 Updates of date picker widgets for temperature (a) and precipitation (b)

(5) Test if the two conditions schemed earlier in user interaction design are checked by the program as expected by creating a timelapse without specifying the spatial extent and creating a timelapse with the start date later than the end date.

Figure 18 Testing of date error warning (a) and missing ROI warning (b)

37

The screenshots in Figure 18 demonstrate the warning from the web app under the two interactive testing cases. The first one is to simulate a situation where the user accidentally enters an end date that is earlier than the start date, with the app giving an expected warning about the error. The second one is a simulation of a case where the user puts all the parameters correctly but forgets to specify the spatial extent of the timelapse, and the web app prompts the user to draw a feature on the map to define the region of interest.

(6) Go through all the datasets with a certain ROI and a set of randomly assigned input parameters such as start date and end date to test if the timelapse can be generated successfully with the expected configuration. For example, Figure 19 shows the result of creating a timelapse for temperature from 2010 to 2020 at a yearly frequency, which is added to the map as an overlay at the correct position. Also, test if the timelapse gif can be saved to the local computer. After this, change all the input parameters, including title, start date, end date, speed, progress bar, font size, font color, and frequency, to test if they are functioning as expected.
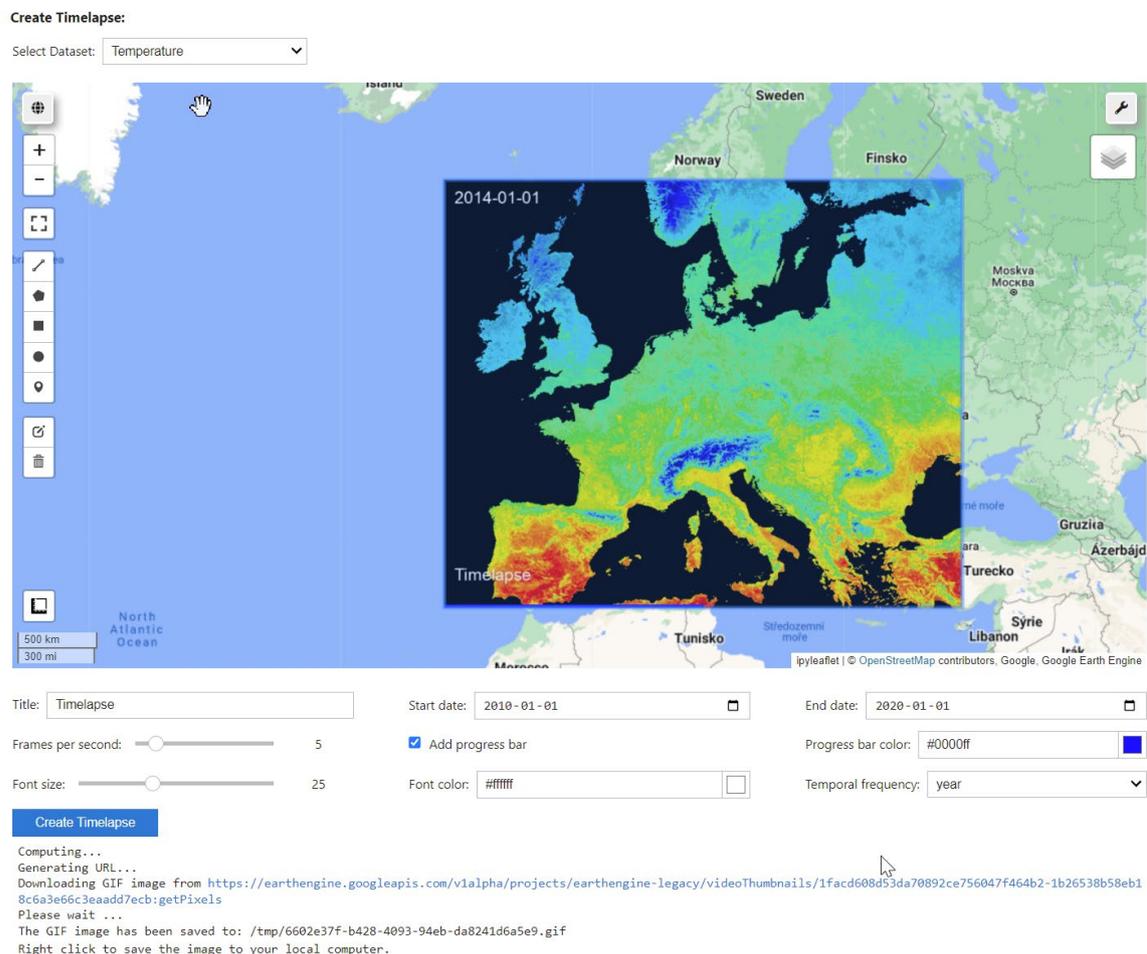
Figure 19 Testing of timelapse generation for yearly mean temperature from 2010 to 2020

(7) For the user guideline section, click on all the hyperlinks one after another to test if they are redirected to the corresponding internet resource.

During the whole process of dynamic testing stated above, all the mismatches and errors are collected and corrected or adjusted later. At this point, there should be no major problems or defects in the EO4BEE web app, which is ready for further user testing.

Refinement to improve user experience

The web app has been tested by three students in the field of geoinformatics, and the feedback from them has been noted and dealt with. Based on the opinions of the users, three major refinements listed below have been applied to the "EO4BEE" web app to improve user experience.

(1) When users click on the hyperlinks, all of them open in the current tab, which would interrupt the current workflow running in the web app. In order to avoid this unpleasant behavior, changes similar to the following example have been made to the markdown codes of all the hyperlinks in the web app.

Before refinement: `[GitHub Repo](https://github.com/YuanWANG2662/EO4BEE-HEROKU.git)`

After refinement: `<a href="https://github.com/YuanWANG2662/EO4BEE-HEROKU.git" target="_blank">GitHub Repo</a>`

(2) As can be seen in the user interface design in Figure 9, the user guidelines section is taking up almost all the space of the browser window, which prevents users from seeing the core functionality of the app at first glance. In order to make sure that users can spot the crucial part of the web app once they enter it, and are still able to read the guidelines before interacting with the app, the information about data sources has been moved to the end of the app. Instead, an anchor was added to allow the user to jump to the details on data sources. Also, sometimes when users do not read through the guidelines carefully, they might not be aware of the existence of the timelapse generator section, which requires scrolling down on the webpage. To solve this, another anchor to jump to the timelapse generator was added and highlighted to grab the user's attention. These two anchors are shown in Figure 20 and are implemented by the markdown codes below:

```
<strong><a href='#data_source'> (See details about the data sources) </a></strong>
<a id='data_source'></a>
<strong>Details about the data source:</strong>
<strong><a href='#timelapse'>(Go to Create Timelapse APP)</a></strong>
<a id='timelapse'></a><br>
<strong>     Create Timelapse:</strong>
```

This webapp provide a tool to visualize various earth observation data to support the decision-making process of beekeeping in Europe | GitHub Repo | Contact Author @Yuan WANG

                                    a.

1. Select the earth observation variable that you want to explore. **(See details about the data sources)**
2. Select the time period that you're interested in.
3. Drag the time slider to visualize the image at a specific time which you want to investigate.
4. Click on the tool button and then the 'i' icon to inspect value at a specific location, or the plot icon to plot the change of the chosen variable over time at a specific location.
5. If you want to visualize the change smoothly as a gif, please use the create timelapse tool to create and download customized timelapse gif.

b. **(Go to Create Timelapse APP)**

Figure 20 Anchor for the data sources (a) and timelapse generator (b)

(3) In the time series visualization part, the speed for the automatic play of the image time series is too fast to wait until the whole image is loaded on the map. After some testing, the time interval of the auto-play is changed from two to five seconds:

```
Map.add_time_slider(collection_yearly_mean,vis_params,'','Time series
of annual average air temperature(℃) at 2m',time_interval=5)
```

4.5.2 Deployment to cloud application platform

The last step in the development of the web application is to publish it to the cloud. In this study, the Heroku platform was used for the deployment of the "EO4BEE" web app. The prerequisites for the deployment are the installations of the Heroku command-line interface and git, after which the steps listed below were followed to build and run the web app in the cloud.

(1) Create a new git repository and add all the files required for the deployment. The directory structure of the repository should be organized as demonstrated in the file tree diagram in Figure 21.

```
.
└── EO4BEE-HEROKU/
    ├── notebooks/
    │   └── eo4bee.ipynb
    ├── Procfile
    ├── requirements.txt
    └── runtime.txt
```
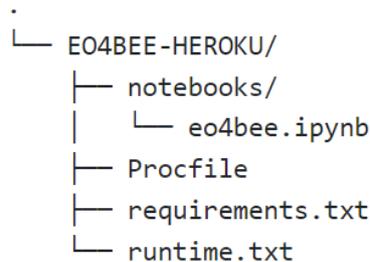
Figure 21 File tree diagram for the EO4BEE web application git repository

The procfile is a text file that defines the commands to be used to launch the app, which is defined as below for the EO4BEE web app. It tells the web browser to run the Jupyter Notebook "eo4bee.ipynb" using Voila and print the exception traceback if errors occur. The most important is that the location of the notebook file has to be specified at the end of the line.

```
web:    voila    --port=$PORT    --Voila.ip=0.0.0.0    --no-browser    --
show_tracebacks=True       --debug       --strip_sources=True       --
enable_nbextensions=True  --MappingKernelManager.cull_interval=60  --
MappingKernelManager.cull_idle_timeout=120 notebooks/eo4bee.ipynb
```

The file "requirements.txt" declares all the Python dependencies needed for the app to build and run. The detail that needs extra attention is the version of the packages, e.g., in this web app, a voila package in a higher version than 0.3.0 and a jinja2 package in version higher than 3.0.3 would lead to the crash of the app.

```
voila==0.3.0
git+https://github.com/YuanWANG2662/geemap.git
pyparsing==2.4.7
httplib2==0.19.1
ffmpeg
jinja2==3.0.3
```

The file "runtime.txt" specifies which runtime Python version to be used, which is set to "python-3.8.8" for this web app.

(2) Create a Heroku account and authenticate Heroku by typing "`$ heroku login`" into the command line interface.

(3) Create a new Heroku app named "EO4BEE" using the command below. When the app is created, a git remote with the same name is also created and associated with the local git repository.

```
$ heroku apps:create eo4bee
```

(4) Set the google earth engine token, which is generated previously during environment setup (see section 4.4.1), as a configuration environment variable in Heroku:

```
$ heroku config:set EARTHENGINE_TOKEN = earth_engine_token
```

(5) Deploy the codes to the Heroku server:

```
$ git push heroku master
```

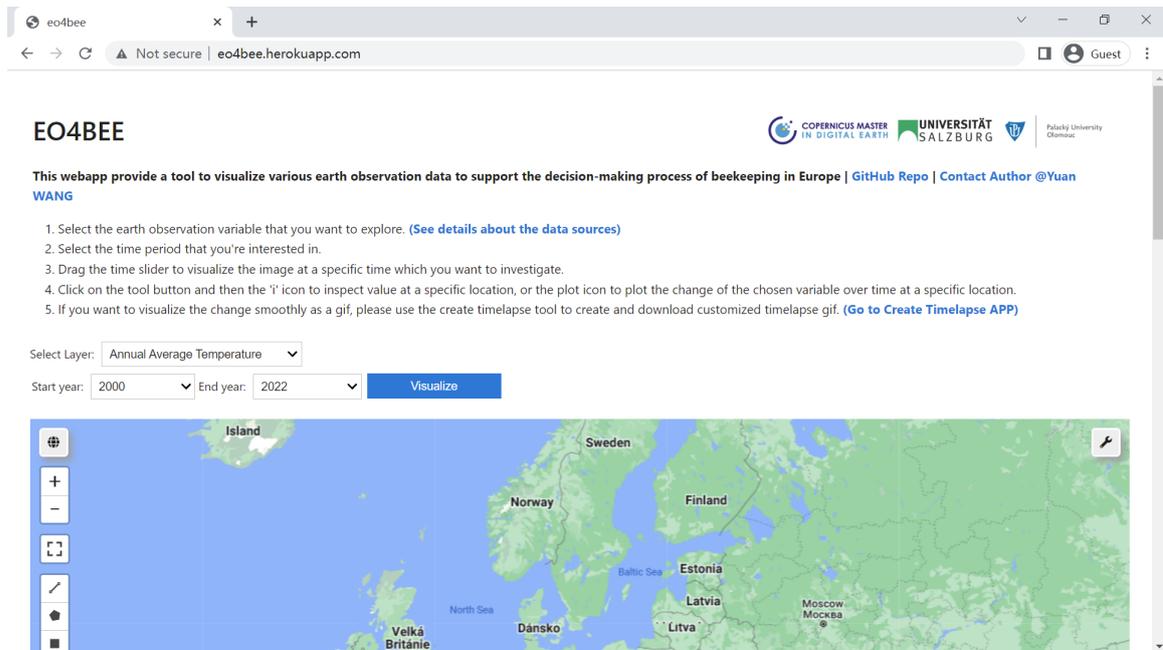At this point, the web application is successfully deployed to Heroku and can be visited through the URL: http://eo4bee.herokuapp.com (Figure 22).

Figure 22 Screenshot of EO4BEE Web Application

5 ASSESSMENT OF LIKELY CLIMATE CHANGE IMPACTS ON BEEKEEPING

5.1 Evaluation of climate change in Europe

5.1.1 Data preprocessing

The data used for the evaluation of climate change in Europe is acquired from the ERA5-Land monthly averaged data, which is part of the Copernicus Climate Change Service (Muñoz-Sabater, 2019). The downloaded dataset is a NetCDF file with the monthly mean air temperature at 2m and precipitation produced by averaging all the daily values, which means the precipitation is not the monthly total but averaged daily total. And this is the reason why the data has to be modified to obtain the monthly total precipitation using the Python script below, the execution of the which requires the installation of the "netCDF4" dependency.

```
import xarray as xr
ds = xr.open_dataset("eu_ precipitation _data.nc").load()
month_length = ds.time.dt.days_in_month
ds1 = ds*month_length
ds1.to_netcdf("precipitation_monthly_sum.nc")
```

After the aggregation, the modified NetCDF file has to be added into ArcGIS Pro and converted to the ESRI multidimensional cloud raster format (CRF) to facilitate further analysis:

(1) In ArcGIS Pro, the option "Multidimensional Raster Layer" was chosen in the "Add Data" dropdown menu to add the multidimensional NetCDF data to the map. As shown in Figure 23, select both "t2m" (air temperature at 2m) and "tp" (aggregated monthly total precipitation) when adding the data.
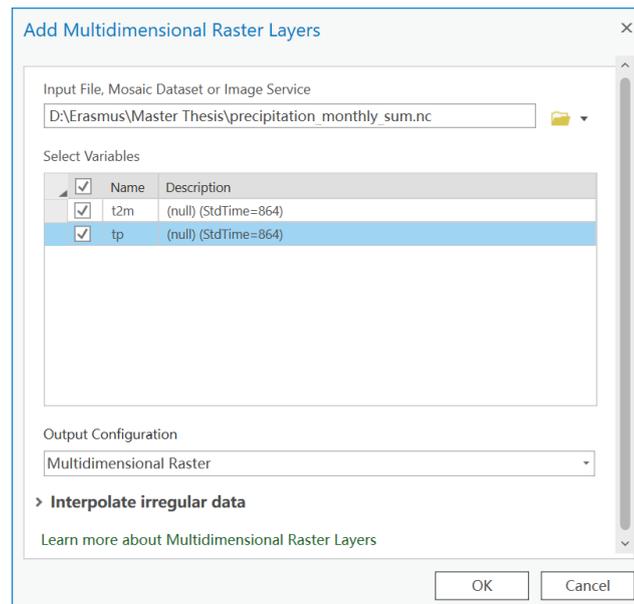

Figure 23 Add NetCDF data as a multidimensional raster layer

(2) Convert NetCDF data into CRF format using the tool "Copy Raster" (Figure 24). The "Build Multidimensional Transpose" is checked to optimize the data processing speed.

When accessing pixel values across all slices in the dataset, the transpose can chunk the multidimensional data along each dimension to improve efficiency. The reason why the data has to be converted is that the CRF format is designed for a large number of slices and faster computing and provides better support for data management and analysis in ArcGIS Pro since CRF is the ESRI native multidimensional raster format.
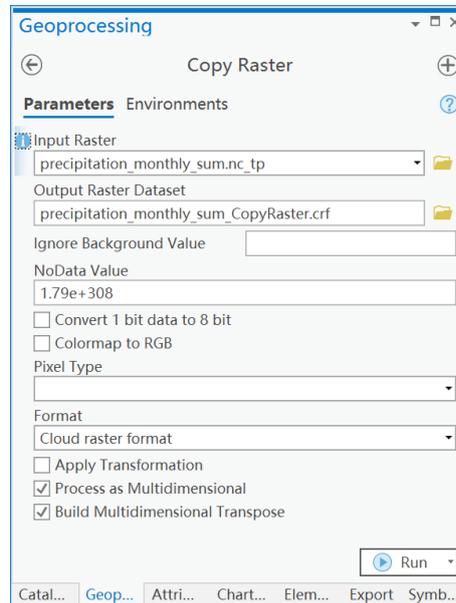

Figure 24 Convert NetCDF data into CRF format

5.1.2 Trend analysis

To evaluate the pattern of likely climate change in Europe, the trends of both annual average temperature and annual total precipitation from 1950 to 2021 were estimated at each pixel from the EO dataset. The first step of the trend analysis is to aggregate the monthly data into yearly data, which can be fitted to a trend line.
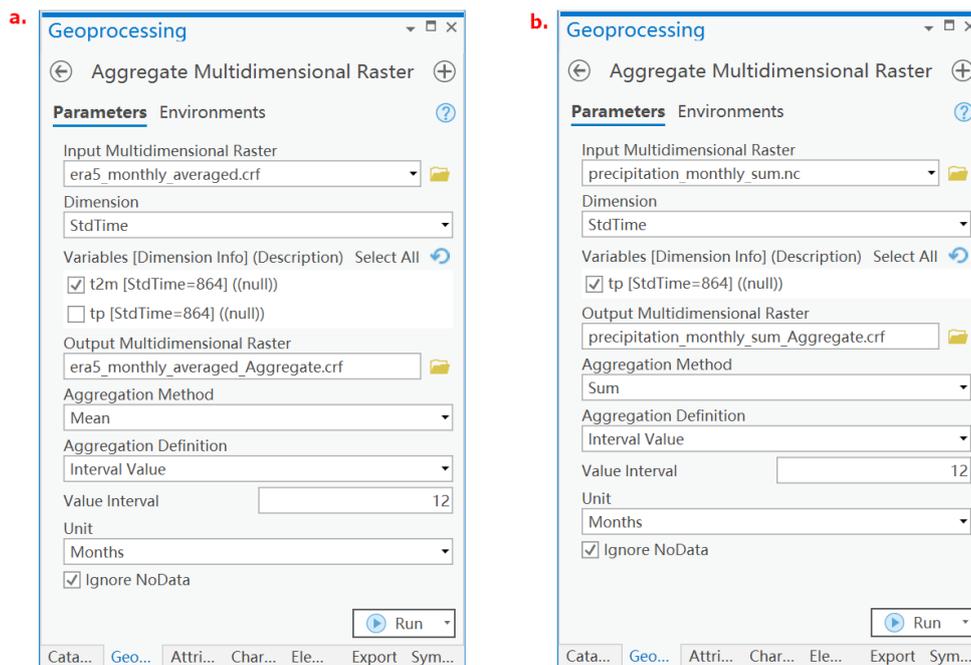
Figure 25 Aggregation for yearly mean temperature (a) and yearly sum precipitation (b)

As displayed in Figure 25, the tool "Aggregate Multidimensional Raster" was applied to temperature and precipitation, respectively. The temperature variable was averaged with a fixed interval of 12 months, and the precipitation variable was summed with the same interval as the temperature, which resulted in two new multidimensional raster datasets: yearly mean temperature and yearly sum precipitation from 1950 to 2021. With the presence of these two datasets, the trend of both temperature and precipitation can be explored in various ways, including plotting the trend for a specific location or region and mapping the trend for the entire area.

The temporal profile charting tool in ArcGIS Pro provides options for creating temporal profiles at a point, along a polyline, or within a polygon for the selected variable in the multidimensional raster. To demonstrate how this can be applied to assist the visualization and evaluation of climate change for a certain region of interest, the temporal profile of both yearly mean temperature and yearly sum precipitation from 1950 to 2021 have been plotted for the Czech Republic (Figure 26).
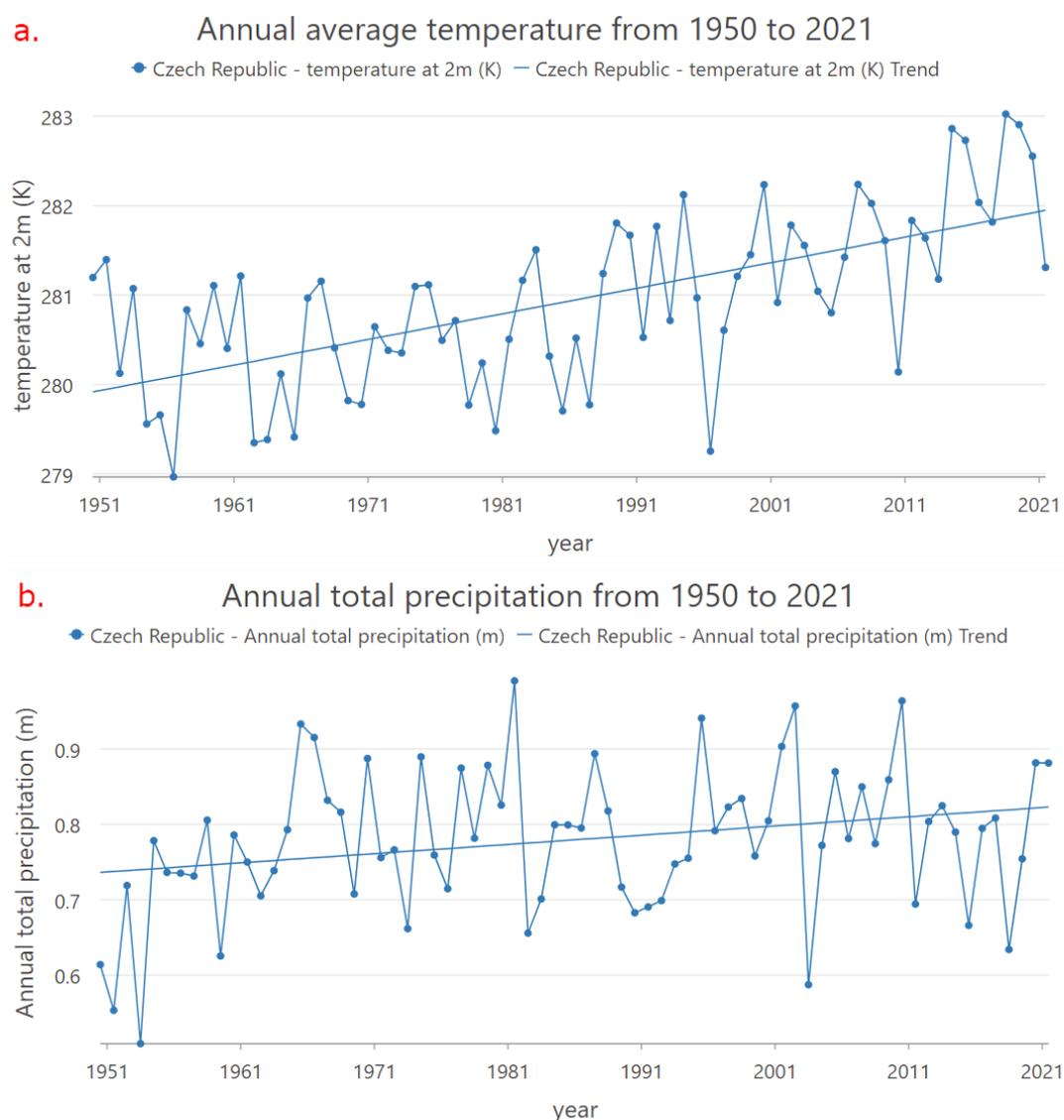

Figure 26 Temporal profile for annual average temperature (a) and annual total precipitation (b) in Czech Republic from 1950 to 2021

The linear regression models for these two temporal profiles are as follows, with model 1 describing the linear trend for the annual average temperature and model 2 for the annual total precipitation.

$$y = 0.000078*x + 278.472023, r^2 = 0.3975259208 \quad (1)$$

$$y = 0.000003*x + 0.674481, r^2 = 0.0707956951 \quad (2)$$

In the Czech Republic example demonstrated above, the increase in temperature from 1950 to 2021 is easily observable. This charting tool can also be applied to any other region of interest for climate change study on a smaller scale.

Except for the investigation at a relatively local scale and with a spatially aggregated metric, the analysis of likely climate change can also be conducted at a larger scale and in a more precise manner, i.e., the trend metric is generated for each pixel instead of being aggregated over a certain area. This is possible using the tool "Generate Trend Raster" in the multidimensional analysis toolset from ArcGIS Pro, which estimates the trend and fits the data along with a linear, polynomial, or harmonic model at each pixel and thus has the capability to reveal where and how the selected variable has changed over a certain time period.
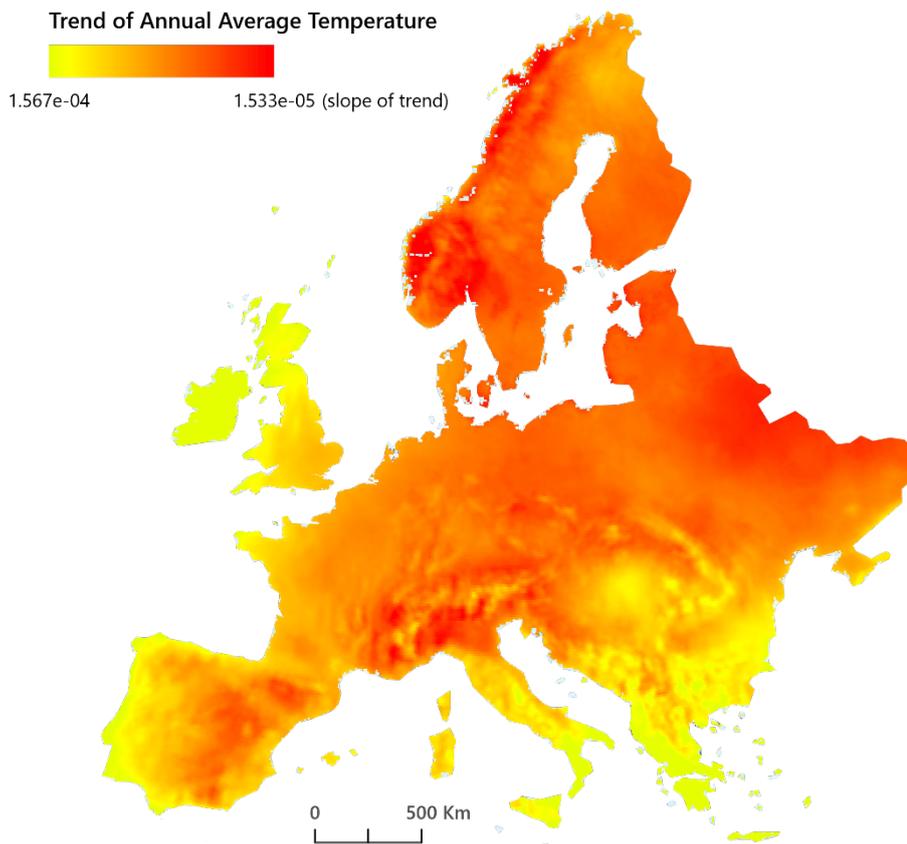

Figure 27 Trend analysis result for annual average temperature from 1950 to 2021 in Europe

In this study, two trend rasters have been generated for the yearly mean temperature (Figure 27) and yearly sum precipitation (Figure 28), respectively, to visualize and analyze the spatial pattern of likely climate change. For the calculation of both trend rasters, the type of trend analysis was set to "linear", which means all the pixel values are fitted along

a linear model. The results of the trend analysis for temperature and precipitation are two multidimensional raster datasets in the CRF format with three bands: slope, intercept, and root mean square error (RMSE). And the slope of the linear trend for each pixel is mapped to describe the direction and extent of temperature change or precipitation change at each location. These two CRF datasets and two trend maps are accessible in the attachment.

The trend analysis result for the annual average temperature provides relatively strong evidence for the large-scale warming of the climate in Europe, with all the pixels indicating a positive trend in temperature change for over 70 years. As shown in Figure 27, the redder the color, the stronger the positive trend in temperature. The regions with a strong positive trend in temperature are the west coast of Norway, southeastern France, northern Italy, eastern Belarus, and northeastern Ukraine; whereas the west coast of Portugal, the south coast of Italy, the north coast of Scotland, and almost the whole state of Greece and Ireland are showing a relatively less strong positive trend in temperature change from 1950 to 2021.
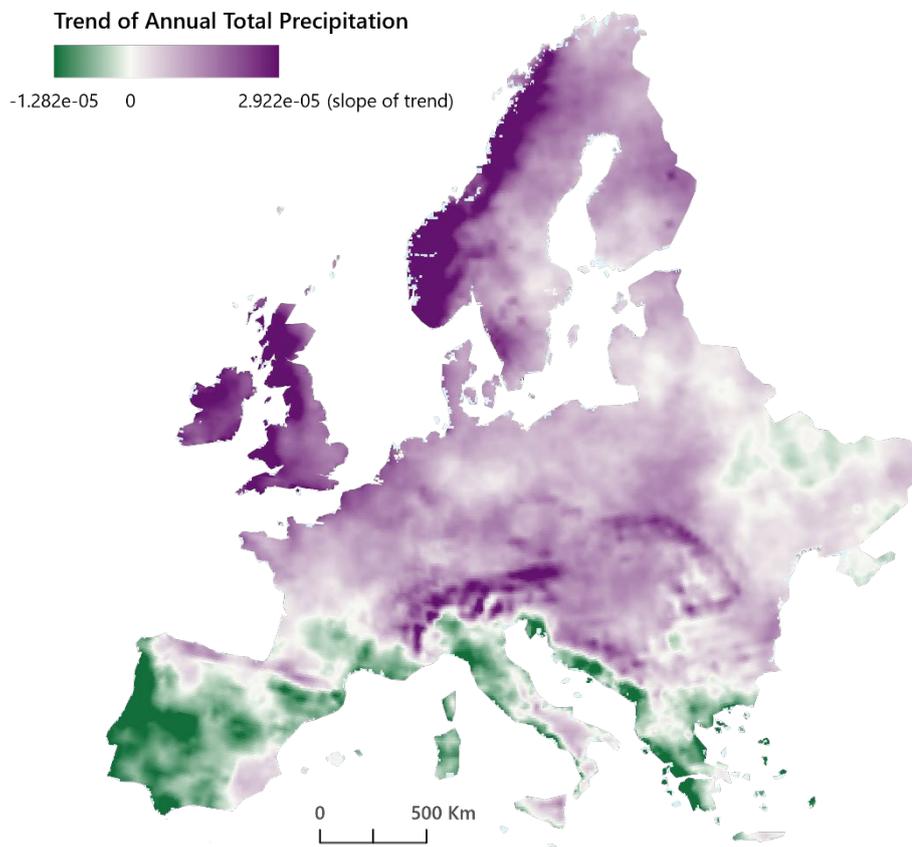
Trend of Annual Total Precipitation

-1.282e-05   0   2.922e-05 (slope of trend)

0   500 Km

Figure 28 Trend analysis result for annual total precipitation from 1950 to 2021 in Europe

The trend analysis result for the yearly total precipitation from 1950 to 2021 shows both positive trends and negative trends in different areas in Europe, and thus is visualized with a bipolar color scheme, with the green color implying a negative trend and the purple color implying the positive trend. It can be observed from Figure 28 that the majority area of Europe, especially the west coast of Norway, the west coast of the United Kingdom, the whole state of Ireland, and the Alpine region are showing a positive trend in annual total precipitation, whereas the state of Portugal, southwestern Spain, northern Italy, and the

south and east coast of the Balkan Peninsula are indicating a negative trend in annual total precipitation from 1950 to 2021.

In order to provide a metric for the tendency of temperature and precipitation change in each state in Europe, zonal statistics have been calculated for 44 countries covered by the trend raster generated previously. The results for both temperature and precipitation are listed in Table 5. Among all these states, Belarus has witnessed the most drastic rising trend of annual average temperature from 1950 to 2021, with the slope of the trend line being 8.76719E-05, whereas Faroes showed the mildest temperature increase with the slope of the trend line being 2.01451E-05. As for the trend of yearly total precipitation, the sharpest drop of precipitation was found in the country of Portugal, with the slope of the trend line being -4.12E-06, whereas Norway demonstrated the most obvious rise in annual total precipitation from 1950 to 2021, with a slope value of 8.53E-06.

Table 5 Slope of the annual average temperature trend and annual total precipitation trend from 1950 to 2021 in 44 countries in Europe

Country	ISO3 code	Temperature trend	Precipitation trend
Albania	ALB	4.03329E-05	-2.70E-06
Andorra	AND	6.51808E-05	5.46E-07
Austria	AUT	7.81442E-05	5.69E-06
Belarus	BLR	8.76719E-05	1.05E-06
Belgium	BEL	7.05635E-05	3.95E-06
Bosnia and Herzegovina	BIH	5.86383E-05	2.24E-06
Bulgaria	BGR	4.58853E-05	9.20E-07
Croatia	HRV	6.63922E-05	1.53E-06
Czechia	CZE	8.04273E-05	3.15E-06
Denmark	DNK	7.29799E-05	3.68E-06
Estonia	EST	8.45635E-05	2.72E-06
Faroes	FRO	2.01451E-05	2.21E-06
Finland	FIN	7.42571E-05	3.11E-06
France	FRA	6.74481E-05	1.60E-06
Germany	DEU	7.7071E-05	2.47E-06
Greece	GRC	3.48998E-05	-2.73E-06
Hungary	HUN	6.12963E-05	4.05E-06
Ireland	IRL	2.3144E-05	7.36E-06
Isle of Man	IMN	3.45835E-05	7.71E-06
Italy	ITA	5.98032E-05	3.00E-07
Jersey	JEY	4.49279E-05	6.51E-06
Latvia	LVA	8.30613E-05	1.76E-06
Liechtenstein	LIE	8.76088E-05	5.86E-06
Lithuania	LTU	8.14383E-05	8.19E-07
Luxembourg	LUX	7.1931E-05	2.97E-06
Malta	MLT	3.67479E-05	-1.50E-06
Moldova	MDA	7.18624E-05	8.63E-07

Table 5 (continued)

Montenegro	MNE	4.92888E-05	-3.24E-07
Netherlands	NLD	6.96301E-05	4.19E-06
North Macedonia	MKD	4.97998E-05	-8.68E-07
Norway	NOR	8.448E-05	8.53E-06
Poland	POL	7.8456E-05	2.52E-06
Portugal	PRT	4.40959E-05	-4.12E-06
Romania	ROU	5.92792E-05	2.34E-06
San Marino	SMR	5.98032E-05	3.00E-07
Serbia	SRB	5.58664E-05	1.71E-06
Slovakia	SVK	7.77245E-05	4.36E-06
Slovenia	SVN	7.56627E-05	2.06E-06
Spain	ESP	6.22837E-05	-1.45E-06
Sweden	SWE	7.81914E-05	3.98E-06
Switzerland	CHE	7.71327E-05	4.95E-06
Ukraine	UKR	7.78148E-05	8.85E-07
United Kingdom	GBR	4.574E-05	7.49E-06
Vatican City	VAT	5.2221E-05	-1.50E-06

5.1.3 Multidimensional principal components analysis

The multidimensional principal components analysis (PCA) is a new feature in ArcGIS Pro 2.9, which can reduce the dimensionality of the data while still preserving most of the information to extract patterns from the image time-series data. The key of PCA is to trade some accuracy for simplicity by projecting the data into a space with reduced dimensions constructed by principal components, where the data can be analyzed and visualized more efficiently, and patterns are much easier to identify.
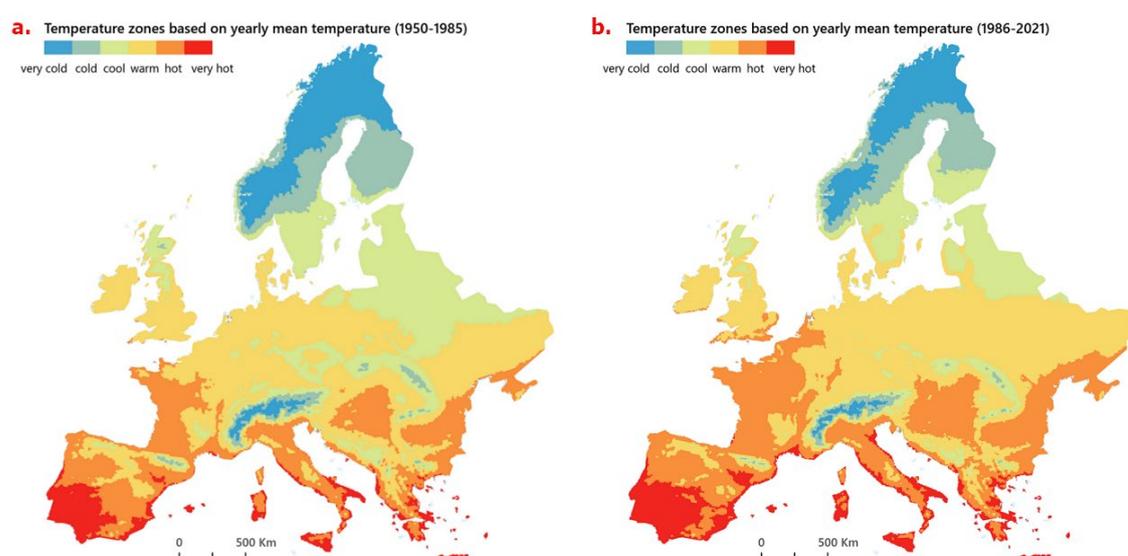

Figure 29 Results of multidimensional PCA for annual average temperature from 1950 to 1985 (a) and from 1986 to 2021 (b)

In this study, the multidimensional PCA has been applied to two image time series of annual average temperature from 1950 to 1985 and from 1986 to 2021, respectively, in order to explore the change of temperature from the perspective of spatial pattern. The number of principal components is set to be automatically computed to be able to explain at least 95% of the variance in the multidimensional raster. The outputs of the PCA contain three files: a raster that stores each computed principal component as a band, a loading table documenting the contribution weight of each raster in the calculation of principal components, and an eigenvalue table indicating the percentage of variance explained by the principal components.

The PCA analysis for both image time series resulted in only one principal component explaining more than 95% of the variance in the data (99.997284% for the image time series from 1950 to 1985 and 99.997969% for the image time series from 1986 to 2021). The loading tables resulting from the analysis are accessible in the attachments. The two raster outputs only have one band since one principal component is sufficient to represent the prevalent spatial pattern in both image time series, and these two raster outputs have been classified using the same data value ranges and visualized as shown in Figure 29. It can be seen that the PCA results are capable of identifying different temperature zones from cold to hot. And in the before and after comparison demonstrated in Figure 29, the expansion from relatively hot areas towards relatively cold areas from the first half to the second half of the time span from 1950 to 2021 can be very easily spotted, especially in regions including southeastern Spain, central France, central and eastern Europe, etc.

5.2 Assessment of likely climate change impacts on beekeeping

The assessment of likely climate change impacts on beekeeping is done only in the state of the Czech Republic as a case study due to the limitation of access to bee colony data. However, the methodologies adopted in this case study case can be easily transplanted to other regions with good data sources, thus providing a new idea for the application of EO data in the study of the impact of likely climate change on the survival of bees.

5.2.1 Data preprocessing

Since the case study is carried out in a region with a much smaller area than in section 5.1, the spatial resolution of the multidimensional raster data used in the previous section is no longer sufficient for this section. Therefore, the temperature data used in this case study is the MODIS Terra Land Surface Temperature and Emissivity dataset (Wan et al., 2015) from NASA with 1 km resolution, and the precipitation data is the TerraClimate global dataset for monthly climate (Abatzoglou et al., 2018) with a spatial resolution of around 4 km.

For the temperature data, because it is not available in the multidimensional raster format required for further analysis, it has to be retrieved from GEE and processed into the correct data format in ArcGIS Pro. Besides, since the MODIS Terra product is a dataset providing daily values, it needs to be aggregated into yearly mean values before being exported from GEE to reduce image size. The following JavaScript code snippet is executed in the GEE online code editor to export 21 images of the yearly mean temperature in the Czech Republic from 2001 to 2021. The reason why the image time series is only starting from 2001 but not earlier is due to the limitation of the data source

time availability, which starts from February 2000 and makes the yearly mean value in 2000 not valid.

```
var years = ee.List.sequence(2001, 2021);
var months = ee.List.sequence(1, 12);
var bbox = ee.Geometry.BBox(11.8, 48.3, 19.3, 51.2);
var collection = ee.ImageCollection('MODIS/006/MOD11A1').select('LST_Day
_1km').filterDate('2001-01-01', '2021-12-31')
var projection = collection.first().projection().getInfo();
var yearly_mean_collection = ee.ImageCollection.fromImages(years.map(
function(y){
  var meanImage = collection.filter(ee.Filter.calendarRange(y, y, 'year')
  ).reduce(ee.Reducer.mean());
  var date = ee.Date.fromYMD(y, 1, 1).format("YYYY_MM_dd");
  meanImage = meanImage.set('system:time_start', ee.Date.fromYMD(y, 1, 1))
  meanImage = meanImage.set('system:index', date)
  return meanImage
}))
var year = 2001
yearly_mean_collection = yearly_mean_collection.sort('system:index')
var image_list = yearly_mean_collection.toList(21)
for (var i = 0; i < 21; i++){
  Export.image.toDrive({
    image: image_list.get(i),
    description: 'yearly_mean_temperature_'+year,
    crs: projection.crs,
    crsTransform: projection.transform,
    region: bbox
  })
  year++
}
```

After these images are exported to Google Drive in TIFF format, they can be downloaded to a local computer, added to a mosaic dataset in ArcGIS Pro, and further converted to a multidimensional raster in CRF format. The processed annual average temperature image time series from 2001 to 2021 is accessible as a multidimensional raster dataset in the attachment.

Concerning the precipitation data, there are already yearly datasets available in NetCDF format from the TerraClimate product (Abatzoglou et al., 2018), which also need to be added to a mosaic dataset in ArcGIS Pro and converted to a single multidimensional raster in CRF format. Moreover, the converted dataset has to be aggregated to get yearly total precipitation since the original dataset contains monthly values. The processed and aggregated annual total precipitation image time series from 2000 to 2020 is accessible as a multidimensional raster in the attachment.

The honey bee colony winter losses data need to be filtered according to the value of representativeness since only representativeness greater than 2% can be considered statistically reliable. The minimum value is calculated from the representativeness values of all the years and used as the metric to filter the dataset using the 2% threshold, which ensures that the selected ZIP code regions have reliable bee colony losses data for all of the years from 2013 to 2020. There are, in total, 162 out of 2665 regions with unique ZIP code filtered from the original dataset.

5.2.2 Trend analysis

The trend analysis in this section basically follows the same procedure as in section 5.1.2, but at a more local scale (in the Czech Republic) and with a more precise resolution, which serves better the accuracy demand in assessing the possible impacts of likely climate change on bee colonies. The results of the trend analysis for annual average temperature and annual total precipitation are shown in Figure 30 and Figure 31, respectively.
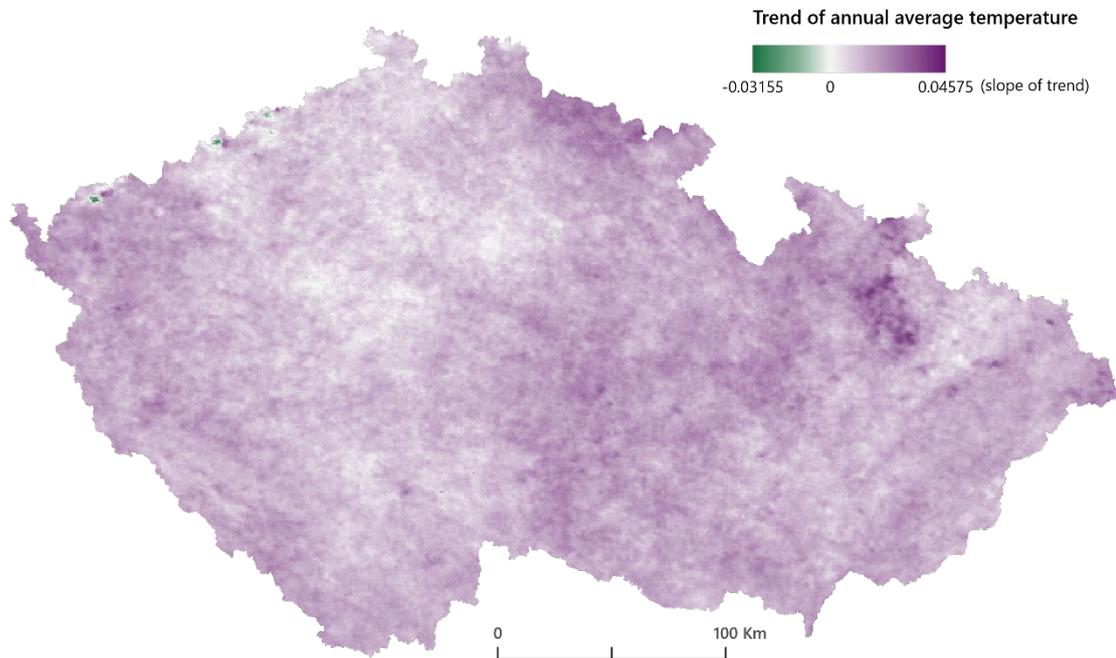

Figure 30 Trend analysis result for annual average temperature from 2001 to 2021 in the Czech Republic
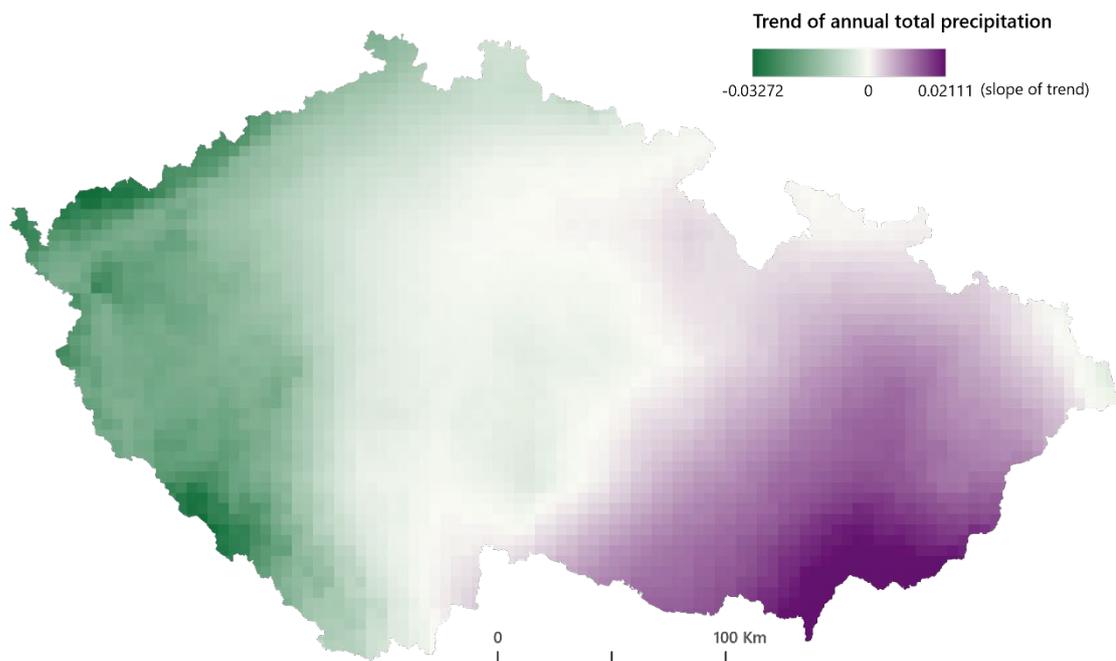
Figure 31 Trend analysis result for annual total precipitation from 2000 to 2020 in the Czech Republic

It can be seen from the result trend map that the vast majority of the area in the Czech Republic shows a positive trend in annual average temperature from 2001 to 2021, except for several very small areas along the northwestern mountains. As for precipitation, the eastern part of the Czech Republic has witnessed a positive trend in the change of yearly total precipitation from 2000 to 2020, whereas the western part, especially the regions along the mountains, are showing a negative trend in annual total precipitation. Trend maps like these can assist beekeepers as well as bee experts in the decision-making process.

Zonal statistics of the temperature trend raster are calculated for the 162 regions with unique ZIP code filtered previously during data preprocessing. The mean values of colony losses percentage are also calculated for the 162 regions. These two tables are joined together using the unique postal code and plotted to explore the correlation between the temperature trend and honey bee colony losses (Figure 32). It can be seen from the scatter plot and the low r^2 (0.0006) of the regression model that no statistically significant correlation was found between the trend of annual average temperature and winter losses of honey bee colonies in this case study.
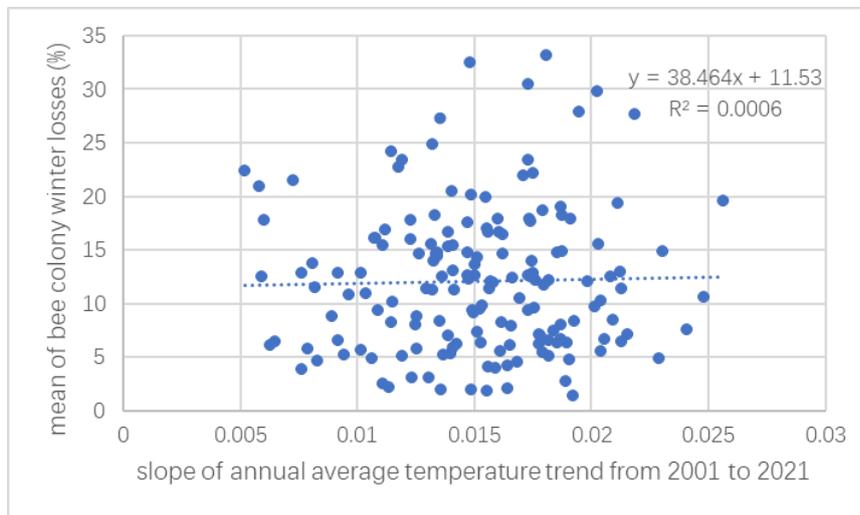

Figure 32 Scatter plot of annual average temperature trend from 2001 to 2021 and mean of bee colony winter losses from 2013 to 2020
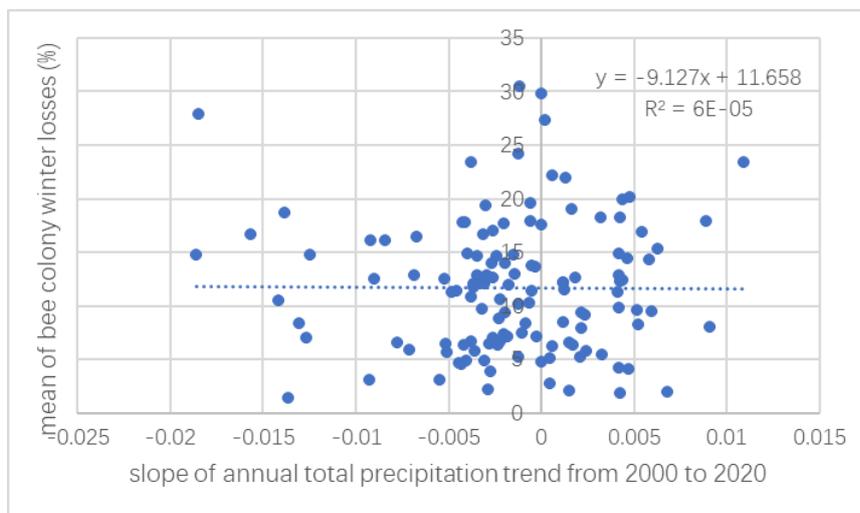

Figure 33 Scatter plot of annual total precipitation trend from 2000 to 2020 and mean of bee colony winter losses from 2013 to 2020

The same procedure was applied for the yearly total precipitation trend (Figure 33), and the result of the r^2 of the regression model is 6E-05, which means the correlation between the mean winter colony losses of the honey bee and the annual total precipitation trend is also not statistically significant in this case study.

5.2.3 Analysis of temperature anomalies and bee colony losses

In order to further explore the relation between temperature and honey bee colony winter losses, the temperature anomalies are analyzed within the 162 regions with valid honey bee colony data. The tool "Generate Multidimensional Anomaly" in ArcGIS Pro offers a convenient method to calculate the anomalies (deviation of an observation from its mean value) for each slice in an image time series. It is applied to the annual average temperature time series from 2001 to 2021, and the result was averaged over the whole area of the 162 valid regions. The winter losses of the honey bee colony are also aggregated into the mean value over the same area for each year from 2013 to 2020. The results are listed in Table 6.

Table 6 Temperature anomalies from 2001 to 2021 and honey bee colony winter losses from 2013 to 2020 in the area of 162 valid regions

Year	Temperature anomaly (K)	Colony winter losses (%)
2001	-2.70747	
2002	-0.47786	
2003	0.99104	
2004	-1.67068	
2005	-1.95994	
2006	-1.28879	
2007	1.73213	
2008	-0.07065	
2009	0.77097	
2010	-1.40244	
2011	-0.34717	
2012	-0.70227	
2013	0.96992	4.106790123
2014	0.16947	14.49938272
2015	1.4457	3.504320988
2016	0.73733	17.48641975
2017	-0.07901	12.05246914
2018	3.14102	12.46296296
2019	1.25216	19.77530864
2020	0.30196	13.01049383
2021	-0.80542	

The evolution of temperature anomalies from 2012 to 2020 and honey bee colony winter losses from 2013 to 2020 are plotted and compared in a combined line chart to explore

the relationship between them (Figure 34). From the combined line chart, it can be noticed that the two lines have a similar shape of fluctuation: both have three peaks, and each peak is higher than the previous one. The peaks for temperature anomalies appear in 2013, 2015, and 2018, whereas the peaks of honey bee colony winter losses are discovered in 2014, 2016, and 2019, which are with exactly one year delay compared to the temperature anomalies. This finding cannot prove that a high temperature anomaly will cause more winter losses of bee colonies but may provide some evidence for the association between rising temperature anomalies and high bee colony winter losses.
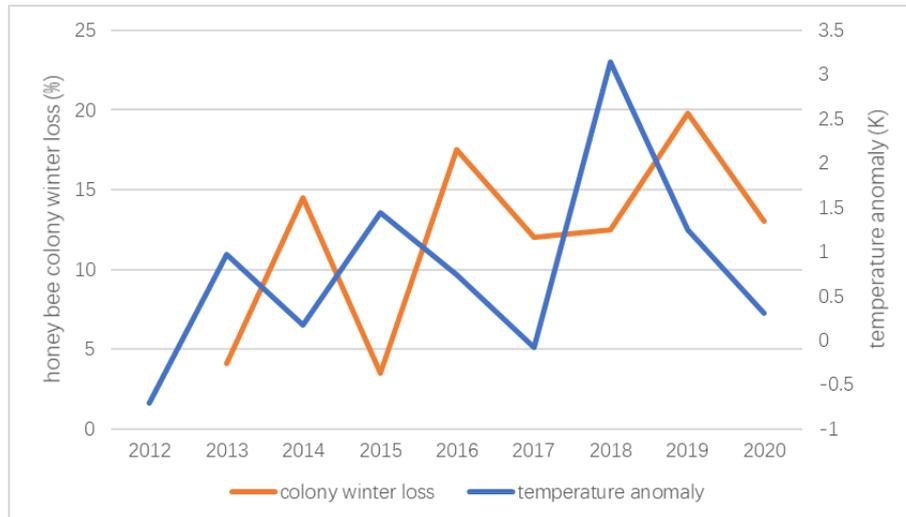
Figure 34 Combined line chart of temperature anomalies from 2012 to 2020 and honey bee colony losses from 2013 to 2020

During the elaboration of this thesis, the bee colony winter losses in some of the regions for the 2011-2022 winter were obtained. The intersection has been made between the 162 regions that have valid data for the previous years and regions that have the latest data, resulting in 111 valid regions. The same procedures of temporal profile analysis are applied, and the results of temperature anomalies from 2012 to 2021 and honey bee winter losses from 2013 to 2021 are aggregated over the area of the 111 valid regions.
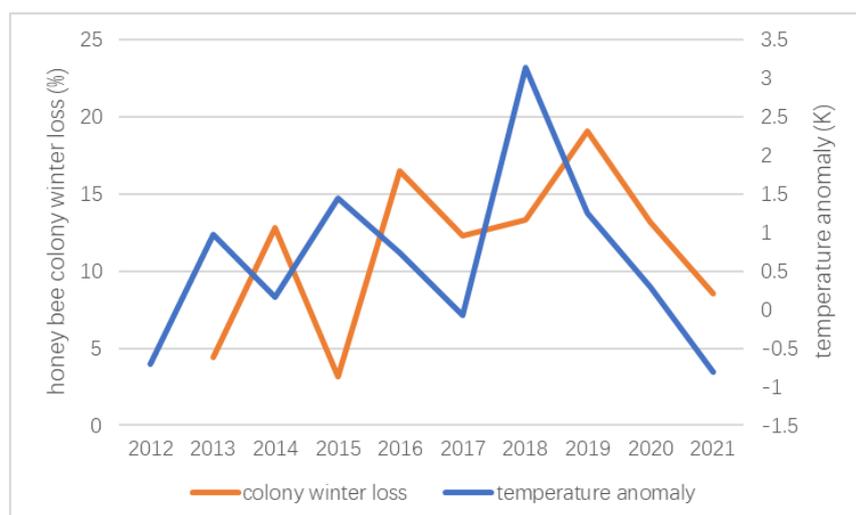

Figure 35 Combined line chart of temperature anomalies from 2012 to 2020 and honey bee colony losses from 2013 to 2020

The two temporal profiles are plotted again to be compared (see Figure 35). It can be seen that the bee colony winter loss for the latest year is still following the fluctuation of the temperature anomaly, which is consistent with our previous findings and strengthens the conjecture. However, it has to be noticed that the trade-off for the data of an extra year is losing almost one-third of the number of sample regions, which would reduce the credibility to some extent. This is why it is more appropriate to still consider Figure 34 as the result of temporal profile analysis.

6 RESULTS

This chapter gives a summary of all the results achieved in this study, which can be divided into two parts: the result of the web application development and the results from the assessment of climate change and its possible impacts on beekeeping. The web application part consists of the web app itself and the outputs from the web app, including maps, animations, and videos. The results from the analysis part are comprised of maps, figures, and tables demonstrating the patterns and statistics of climate change in Europe as well as the possible association between climate change and beekeeping.

6.1 Results of EO4BEE web application

The web application named "**EO4BEE**" was developed using the GEE Python API (see subchapter 4.4) based on the big repository of publicly available EO data and the strong cloud-computing power of GEE and was published on the Heroku cloud platform at the URL: http://eo4bee.herokuapp.com (see subchapter 4.5).

The EO4BEE web app managed to empower the visualization of EO variables related to the living environment of bees not only at a large spatial scale but also over a long time span. It consists of four sections (see attachment 3), user guidelines section, time-series visualization section, timelapse generator section, and the data sources reference section. The user guidelines give an overview of the web app and instructions on how to utilize it. The time series visualization section makes it possible to investigate the spatiotemporal pattern of the EO variables through a time slider, inspect exact values at a specific location or area of interest using the inspector, and explore the evolution of a certain variable over time using the plotting tool. Although it is feasible to play the image time series one after another automatically in the time series visualization section, the display of these images is not continuous because the requests of images are real-time, which means it may take a few seconds for an image to load. The timelapse generation section makes up for this defect and allows continuous visualizations of image time series in the form of animations, thus providing users with a more intuitive and smoother overview of the change of EO variables. The details and sources of all the data involved in the previous sections are listed in the last part of the web app.

Except for the EO4BEE web app itself, the results also include the outputs such as maps, figures, and animations that are generated from EO4BEE. The number of these outputs can be unlimited since they are highly customized based on the interest of the users. Two demo time-lapses showing the annual average temperature from 2001 to 2020 and yearly total precipitation from 1958 to 2020 in Europe are included in the attachments.

6.2 Results of climate change analysis in Europe

The patterns of climate change in Europe were analyzed and visualized from the time series of annual average temperature data and annual total precipitation data from 1950 to 2021. Tools in the multidimensional analysis toolset in ArcGIS Pro, including "Create Temporal Profiles", "Generate Trend Raster", and "Multidimensional Principal Components Analysis", have been applied to the dataset to calculate the results.

The results from the trend analysis contain figures, trend raster, maps, and statistic tables. The two temporal profiles of the annual average temperature and yearly total precipitation from 1950 to 2021 (see Figure 26) were plotted for the Czech Republic as an example demonstrating how multidimensional raster data can be used to explore the

evolution of the selected variable over time in any region of interest. The two trend raster output datasets were calculated within every pixel in the multidimensional raster to fit a linear trend model for yearly mean temperature and yearly total precipitation, respectively. These two datasets are included in the attachments, and the slope value of the temperature trend as well as the precipitation trend was visualized in two trend maps (see Figure 27 and Figure 28). In the temperature trend map, it can be easily observed that all the pixels are showing a positive trend in annual average temperature from 1950 to 2021, which can provide strong evidence for the warming of the climate in Europe. The regions that have a relatively steep slope in the rising trend are the west coast of Norway, northern Italy, southeastern France, northeastern Ukraine, and eastern Belarus; and a relatively mild changing trend was found on the south coast of Italy, the west coast of Portugal, the north coast of Scotland, and almost the whole state of Ireland and Greece. As for precipitation, the trend map indicates that most areas of Europe witnessed a positive trend in annual total precipitation, especially in the Alpine region, the west coast of the United Kingdom, the west coast of Norway, and the whole country of Ireland; but northern Italy, southwestern Spain, the whole state of Portugal, and the south and east coast of the Balkan Peninsula had a decreasing trend in annual precipitation from 1950 to 2021. The zonal statistics of both the temperature trend and the precipitation trend have also been calculated and summarized for 44 countries covered in the study area (see Table 5). These results from trend analysis can give clues for predicting which regions might need extra attention in bee conservation.

The results from the multidimensional principal components analysis are two raster datasets that store the principal components calculated for the time series of annual average temperature in two 36-year periods (1950-1985 and 1986-2021). Except for these two raster datasets, two loading tables containing the weight for each time slice and two eigenvalue tables indicating the percentage of variance explained by each principal component are also generated from the analysis. All of these six output files are included in the attachments. The PCA analysis for the two time periods both ended up with only one principal component, which explains 99.997284% and 99.997969% of the variance in the time series data for 1950-1985 and 1986-2021, respectively. The two principal components of raster datasets were classified and visualized with the same data ranges (see Figure 29) to establish a before-after comparison of the temperature distribution pattern in Europe. And the expansion of hot zones towards cold zones was identified in various regions, including central France, southeastern Spain, central and eastern Europe, etc., which can affect the living conditions in bee habitats.

6.3 Results of association analysis between climate change and beekeeping

The assessment of likely climate change impacts on beekeeping was carried out in the Czech Republic with the annual average temperature data from 2001 to 2021, the yearly total precipitation data from 2000 to 2020, and the bee colony winter loss data from 2013 to 2020. Trend analysis was applied to the time series of temperature and precipitation data again with a finer spatial resolution (1km for temperature and 4km for precipitation), and two trend raster datasets were calculated and visualized with a bipolar color scheme (see Figure 30 and Figure 31). The results indicate that almost the whole area of the Czech Republic shows a rising trend in annual average temperature from 2001 to 2021, with a few exceptional areas located along the northwestern mountains; and the yearly total precipitation in the eastern Czech Republic has a positive trend from 2000 to 2020,

while the western part of the country showed a downward trend. Based on the zonal statistics calculated from the trend analysis results, regression analysis was conducted for 162 districts with valid bee colony data to explore how bee colony winter losses are related to the temperature trend or the precipitation trend. The results for the regression analysis between bee colony winter loss and annual average temperature trend and between bee colony winter loss and annual total precipitation trend both didn't show a statistically significant correlation (see Figure 32 and Figure 33). However, by calculating and plotting the temporal profiles of the yearly temperature anomalies and the yearly bee colony winter losses aggregated over the 162 districts with valid data, it is discovered that the fluctuations in bee colony winter losses have a similar pattern to the variation in temperature anomalies with one year delay(see Figure 34): the temperature anomalies had three peaks in 2013, 2015 and 2018, while the peaks of honey bee colony winter losses can be observed in 2014, 2016 and 2019, and for both temperature anomaly and honey bee colony winter loss, each of the three peaks is higher than the previous one.

7 DISCUSSION

Technical difficulties in EO4BEE web application development

The main difficulty in the realization of the functionalities of the EO4BEE web application lies in the demand for managing, querying, and rendering a massive amount of EO data on the fly, where the features of Google Earth Engine, including the huge public data archive and the powerful cloud-computing ability, are proved to be an excellent resolution. The initial technical framework selected for this web app was to use the GEE JavaScript API for interaction with the earth observations, HTML for structuring, and CSS for styling, which requires fairly advanced command of web development skills to implement all the details manually. However, a Python package named geemap, which is aimed at interactive mapping with GEE, has made the whole development process much more friendly to non-professional web developers. This Python package was built with ipyleaflet and ipywidgets, which makes the interaction design more intelligent for the analysis and visualization of GEE datasets. And this is why I finally decided to switch from JavaScript to Python and developed all the core functionalities of the EO4BEE web application using the APIs from the geemap package, despite the fact that the GEE JavaScript API is better documented.

The implementation of the web app was relatively smooth, whereas the deployment to the cloud can be very tricky. The Heroku PaaS was used in this study to run the application in the cloud, and the deployment can fail easily when a tiny detail is not coordinated. For example, a voila package with a version later than 0.3.0 and a jinja2 package versioned later than 3.0.3 will lead to a crash of the deployed web app. Therefore, the versions of the Python packages require extra specifications during the deployment. In addition, a procfile with even one space character missing can also cause failure, which is a reminder that all details matter in application development.

Data suitability

The EO data used in this diploma thesis is all open source, which largely simplified the process of data retrieval and acquisition. In this study, the two most important dimensions of these datasets are spatial availability and time availability. Spatial availability can be evaluated in two aspects: spatial resolution and spatial coverage. All the EO datasets involved in this thesis have global coverage, which means the study area (Europe) is fully covered. The spatial resolution of these datasets ranges from 30 m (the Landsat 7 Collection 1 NDVI Composite) to 44528 m (The Copernicus Atmosphere Monitoring Service), which can all give a fairly satisfactory visualization result at the scale of Europe. As for the analysis at the scale of the Czech Republic, the datasets with a finer spatial resolution were used: MODIS Terra Land Surface (1000 m) for temperature and TerraClimate (4000 m) for precipitation. Similarly, temporal resolution and the time span coverage are the two aspects to be assessed in time availability. The temperature and precipitation time series datasets used in the multidimensional raster analysis have monthly values, which meet the requirements since the yearly aggregates needed for the trend analysis can be easily calculated. Most of the datasets used in the web app have a sufficient temporal resolution that varies from hourly to monthly, with only one exception being the Copernicus CORINE Land Cover, which has an update cycle of approximately six years. There are also landcover datasets with annual updates, such as the Copernicus Global Land Serve (CGLS), but it only starts in 2015, while the CORINE land cover starts from 2000. And this is why I had to trade some time resolution for time span coverage since this study focuses more on the change in the earth's surface. The time-span

coverage is a very crucial dimension of data in the assessment of likely climate change, and it should be as long as possible. The climate data used to analyze the patterns of climate change in Europe is the ERA5 product from the Copernicus Climate Change Service, covering the time period from 1950 to 2021. However, when integrating climate data with bee colony data in the Czech Republic, MODIS Terra Land Surface and TerraClimate were used instead for their finer spatial resolution, despite the fact that the time period covered is shorter than ERA5. As discussed above, the choice of EO datasets is the result of balancing the demands from various perspectives.

The bee colony winter loss data used in this diploma thesis is crowdsourced from beekeepers all over the Czech Republic based on a citizen science approach. It has been filtered using the percentage of representativeness calculated from the beehive numbers investigated by COLOSS and the beehive data provided by the Ministry of Agriculture of the Czech Republic. Only the data with representativeness greater than 2% is considered valid to be used in this study. This threshold selected 162 out of 2665 data records, which has greatly improved the reliability of the data but also sacrificed the integrity of the bee colony data to a certain extent, which might be one of the reasons for the result of very low r^2 values in the regression analyses (see subchapter 5.2.2). The disadvantages of crowdsourcing, such as lack of precision, are also issues that could affect the results of the analysis. Nevertheless, these deficiencies in bee data do not prevent this study case from providing a very valuable reference for future research that may have more precise data.

Potential and limitations of EO data in beekeeping support

There are still some limitations of EO data in the context of beekeeping support. As a type of insect, bees are in very small size, which makes them basically impossible to be captured in remote sensing images. Therefore, it is impractical to monitor the bees directly, and the influence on bees can only be speculated through indirect means of studying the surrounding environment of bees in satellite images, which cannot be as precise as taking direct measurements from beehives and the fields where the bees are active. Furthermore, although climate variables such as temperature and precipitation and vegetation indicators like NDVI that can affect the living conditions of bees are easily accessible from earth observations, there are still factors that make a big difference to the survival of bees but are not feasible to be observed from the space, for example, floral resources, pesticide use, invasive species, parasite, etc.

Despite the weaknesses stated above, the application of EO data in beekeeping is still a great innovation and advancement. The major advantage EO data have over traditional data measurements is that it can break through the limitations of both spatial and temporal scales. The conventional on-site data collection method requires a lot of time and money and thus is difficult to be carried out at a large scale or for a continuous long time period; However, the satellites can make systematic and regular observations over large areas, contributing a lot to the monitoring of global climate and the earth's surface, which are closely related to the living conditions of bees. This advancement is also reflected multiple times in this study. The temperature and precipitation trend maps from 1950 to 2021 in Europe demonstrated where and how the climate has changed, which can provide valuable information for decision-makers, including bee experts and beekeepers who are familiar with the environmental preferences of various bee species. For instance, if a certain bee species is proved to have a higher mortality rate when the temperature rises, then the areas with a steeply rising trend of temperature in the trend map may require extra attention, and corresponding protective measures can be adopted.

Besides, with the time series of climate data at hand, it is also feasible to make predictions to alert beekeepers of possible anomalies and take precautions for the benefit of bees. To conclude, the multidimensional raster analysis methods applied to the climate data obtained from EO are very enlightening. They can be easily extended to other EO variables related to bee health or even used to establish multi-factor evaluation indicators, which suggests that EO technologies have a rather optimistic application prospect in the context of bee conservation and beekeeping support.

8 CONCLUSION

The principal aim of this diploma thesis was to explore the potential of EO data in the context of beekeeping and likely climate change. The practical objective was to develop a web application for beekeeping support by utilizing the strong cloud computing power and huge EO data catalog of GEE. And the methodological objectives were to extract the spatial patterns of likely climate change in Europe from multidimensional raster obtained by EO, to evaluate the possibility of integrating crowdsourced bee colony data with relevant EO data, and to explore how the analysis results can benefit beekeeping research.

To achieve the practical goal of this study, a web application named "**EO4BEE**" has been developed using the geemap Python package and the Google Earth Engine Python API in Jupyter Notebook. The web app was deployed to the Heroku cloud platform and is available at the URL: http://eo4bee.herokuapp.com. It managed to enable the time-series visualization of EO variables that might have an impact on bee health based on the implementation of a time slider and allow users to generate timelapse to have an overview of the changing pattern of the selected variable. The visualization results from the web app can provide convenience for beekeepers and bee experts during the examination of local living conditions and the environment for bees so that they can make more informed decisions.

In terms of methodological objectives, several multidimensional raster analyses have been applied to the time series raster datasets of temperature and precipitation in ArcGIS Pro to investigate the patterns of likely climate change, the results of which were further integrated with bee colony winter loss data to assess the possible impacts climate change has on beekeeping. The study area is Europe, where the trend raster was calculated and visualized for both annual average temperature and annual total precipitation from 1950 to 2021. The results indicated that the whole study area demonstrated a rising trend in temperature, which provides strong evidence for the warming of the climate, whereas the annual total precipitation didn't show a consistent direction of change in Europe. The statistics for the temperature trend and the precipitation trend have also been calculated and summarized for 44 countries covered by the study area in a result table. Due to the limited availability of bee colony data, the area was limited to the Czech Republic when analyzing the integration of climate data and bee colony winter losses. Regression analyses were performed to study the relationship between bee colony winter loss and temperature trend and between bee colony winter loss and precipitation trend. Although no statistically significant correlations were found for both of them, the methodologies applied in the analysis can still produce new inspiration from EO in the research on beekeeping with concerns of climate change. Furthermore, the time profiles were plotted for bee colony winter losses and temperature anomalies calculated for every year from 2012 to 2020, and similar patterns of fluctuation were discovered from the comparison: the changing pattern of bee colony winter losses basically followed the evolution of temperature anomalies but with exactly one year delay, which indicates that high bee colony winter loss can be associated with high temperature anomalies.

In conclusion, this study provided a new perspective for beekeeping support research in the context of likely climate change, namely the application of EO data. The methodologies applied in this thesis can be easily transplanted to any region of interest, any other observation variables such as NDVI, or even any specific bee species, to study the influence of the changing earth's surface on bee survival.

REFERENCES AND INFORMATION SOURCES

Abatzoglou, J. T., Dobrowski, S. Z., Parks, S. A., & Hegewisch, K. C. (2018). TerraClimate, a high-resolution global dataset of monthly climate and climatic water balance from 1958-2015. Scientific data, 5, 170191. https://doi.org/10.1038/sdata.2017.191

Abou-Shaara, H. F. (2013). Using geographical information system (GIS) and satellite remote sensing for understanding the impacts of land cover on apiculture over time. International Journal of Remote Sensing Applications, 3(4), 171-174.

Alhaddad, S., & Darchen, B. (1995). The influence of meteorological conditions on the feeding and egg laying of the queen honey bee [Apis mellifera ligustica]. *Comptes Rendus de l'Academie des Sciences Serie 3 Sciences de la Vie (France).*

Amani, M., Ghorbanian, A., Ahmadi, S. A., Kakooei, M., Moghimi, A., Mirmazloumi, S. M., ... & Brisco, B. (2020). Google earth engine cloud computing platform for remote sensing big data applications: A comprehensive review. IEEE Journal of Selected Topics in Applied Earth Observations and Remote Sensing, 13, 5326-5350.

Amani, M., Mahdavi, S., Afshar, M., Brisco, B., Huang, W., Mohammad Javad Mirzadeh, S., ... & Hopkinson, C. (2019). Canadian wetland inventory using Google Earth Engine: The first map and preliminary results. Remote Sensing, 11(7), 842.

Benedetti, A., Morcrette, J. J., Boucher, O., Dethof, A., Engelen, R. J., Fisher, M., ... & Suttie, M. (2009). Aerosol analysis and forecast in the European centre for medium-range weather forecasts integrated forecast system: 2. Data assimilation. Journal of Geophysical Research: Atmospheres, 114(D13). https://doi.org/10.1029/2008JD011115

Bommarco, R., Lundin, O., Smith, H. G., & Rundlöf, M. (2012). Drastic historic shifts in bumble-bee community composition in Sweden. Proceedings of the Royal Society B: Biological Sciences, 279(1727), 309-315.

Bontemps, S., Herold, M., Kooistra, L., Van Groenestijn, A., Hartley, A., Arino, O., ... & Defourny, P. (2012). Revisiting land cover observation to address the needs of the climate modeling community. Biogeosciences, 9(6), 2145-2157.

Brodschneider, R., Brus, J., & Danihlík, J. (2019). Comparison of apiculture and winter mortality of honey bee colonies (Apis mellifera) in Austria and Czechia. Agriculture, Ecosystems & Environment, 274, 24-32.

Brodschneider, R., Gray, A., Adjlane, N., Ballis, A., Brusbardis, V., Charrière, J. D., ... & Danihlík, J. (2018). Multi-country loss rates of honey bee colonies during winter 2016/2017 from the COLOSS survey. Journal of Apicultural Research, 57(3), 452-457.

Brodschneider, R., Gray, A., & COLOSS Monitoring Core Project#. (2022). How COLOSS monitoring and research on lost honey bee colonies can support colony survival. Bee World, 99(1), 8-10.

Brodschneider, R., Gray, A., Van der Zee, R., Adjlane, N., Brusbardis, V., Charrière, J. D., ... & Woehl, S. (2016). Preliminary analysis of loss rates of honey bee colonies during winter 2015/16 from the COLOSS survey. Journal of Apicultural Research, 55(5), 375-378.

Brosi, B. J., Daily, G. C., Shih, T. M., Oviedo, F., & Durán, G. (2008). The effects of forest fragmentation on bee communities in tropical countryside. Journal of Applied Ecology, 45(3), 773-783.

Brown, M. J., & Paxton, R. J. (2009). The conservation of bees: a global perspective. Apidologie, 40(3), 410-416.

Bunting, E. L., Munson, S. M., & Bradford, J. B. (2019). Assessing plant production responses to climate across water-limited regions using Google Earth Engine. Remote Sensing of Environment, 233, 111379.

Burrill, R. M., & Dietz, A. (1981). The response of honey bees to variations in solar radiation and temperature. Apidologie, 12(4), 319-328.

Cameron, S. A., & Sadd, B. M. (2020). Global trends in bumble bee health. Annual review of entomology, 65, 209-232.

Chanthadavong, A. (2021, April 16). Google introduces Timelapse to Google Earth. ZDNet. https://www.zdnet.com/article/google-introduces-timelapse-to-google-earth/

Chapman, J. W., Drake, V. A., & Reynolds, D. R. (2011). Recent insights from radar studies of insect flight. Annual review of entomology, 56, 337-356.

Cox, H., Kelly, K., & Yetter, L. (2014). Using remote sensing and geospatial technology for climate change education. Journal of Geoscience Education, 62(4), 609-620.

Genersch, E. (2010). Honey bee pathology: current threats to honey bees and beekeeping. Applied microbiology and biotechnology, 87(1), 87-97.

Crailsheim, K. (2007). HoPoMo: A model of honeybee intracolonial population dynamics and resource management. *Ecological modelling, 204*(1-2), 219-245.

Gray, A., Adjlane, N., Arab, A., Ballis, A., Brusbardis, V., Charrière, J. D., ... & Brodschneider, R. (2020). Honey bee colony winter loss rates for 35 countries participating in the COLOSS survey for winter 2018–2019, and the effects of a new queen on the risk of colony winter loss. Journal of Apicultural Research, 59(5), 744-751.

Gray, A., Brodschneider, R., Adjlane, N., Ballis, A., Brusbardis, V., Charrière, J. D., ... & Soroker, V. (2019). Loss rates of honey bee colonies during winter 2017/18 in 36 countries participating in the COLOSS survey, including effects of forage sources. Journal of Apicultural Research, 58(4), 479-485.

Dew, R. M., Silva, D. P., & Rehan, S. M. (2019). Range expansion of an already widespread bee under climate change. Global Ecology and Conservation, 17, e00584.

Fawzy, S., Osman, A. I., Doran, J., & Rooney, D. W. (2020). Strategies for mitigation of climate change: a review. Environmental Chemistry Letters, 18(6), 2069-2094.

Flores, J. M., Gil-Lebrero, S., Gámiz, V., Rodríguez, M. I., Ortiz, M. A., & Quiles, F. J. (2019). Effect of the climate change on honey bee colonies in a temperate Mediterranean zone assessed through remote hive weight monitoring system in conjunction with exhaustive colonies assessment. Science of the Total Environment, 653, 1111-1119.

Galbraith, S. M., Vierling, L. A., & Bosque-Pérez, N. A. (2015). Remote sensing and ecosystem services: current status and future opportunities for the study of bees and pollination-related services. Current Forestry Reports, 1(4), 261-274.

Giannini, T. C., Acosta, A. L., Garófalo, C. A., Saraiva, A. M., Alves-dos-Santos, I., & Imperatriz-Fonseca, V. L. (2012). Pollination services at risk: Bee habitats will decrease owing to climate change in Brazil. Ecological Modelling, 244, 127-131.

Gorelick, N., Hancher, M., Dixon, M., Ilyushchenko, S., Thau, D., & Moore, R. (2017). Google Earth Engine: Planetary-scale geospatial analysis for everyone. Remote sensing of Environment, 202, 18-27.

Guo, H., Wang, L., Chen, F., & Liang, D. (2014). Scientific big data and digital earth. Chinese science bulletin, 59(35), 5066-5073.

Hillmann, R. C. (1972). BIOLOGICAL EFFECTS OF AIR POLLUTION ON INSECTS, EMPHASIZING THE REACTIONSOF THE HONEY BEE (APIS MELLIFERA, L.) TO SULFUR-DIOXIDE. The Pennsylvania State University.

Hallmann, C. A., Sorg, M., Jongejans, E., Siepel, H., Hofland, N., Schwan, H., ... & de Kroon, H. (2017). More than 75 percent decline over 27 years in total flying insect biomass in protected areas. PloS one, 12(10), e0185809.

Hersbach, H., Bell, B., Berrisford, P., Biavati, G., Horányi, A., Muñoz Sabater, J., Nicolas, J., Peubey, C., Radu, R., Rozum, I., Schepers, D., Simmons, A., Soci, C., Dee, D., Thépaut, J-N. (2019). ERA5 monthly averaged data on single levels from 1979 to present. Copernicus Climate Change Service (C3S) Climate Data Store (CDS). https://doi.org/10.24381/cds.f17050d7

Hillmann, R. C. (1972). BIOLOGICAL EFFECTS OF AIR POLLUTION ON INSECTS, EMPHASIZING THE REACTIONSOF THE HONEY BEE (APIS MELLIFERA, L.) TO SULFUR-DIOXIDE. The Pennsylvania State University.

Hofmann, M. M., Fleischmann, A., & Renner, S. S. (2018). Changes in the bee fauna of a German botanical garden between 1997 and 2017, attributable to climate warming, not other parameters. Oecologia, 187(3), 701-706.

Huntington, J. L., Hegewisch, K. C., Daudert, B., Morton, C. G., Abatzoglou, J. T., McEvoy, D. J., & Erickson, T. (2017). Climate engine: Cloud computing and visualization of climate and remote sensing data for advanced natural resource monitoring and process understanding. Bulletin of the American Meteorological Society, 98(11), 2397-2410.

IPCC (2007). In: Solomon SD, Qin M, Manning Z, Chen M, Marquis KB, Averyt M, Tignor, Miller HL (eds) Climate change 2007: The physical science basis. Cambridge University Press, Cambridge, United Kingdom and New York, United States.

Jarnevich, C. S., Esaias, W. E., Ma, P. L., Morisette, J. T., Nickeson, J. E., Stohlgren, T. J., ... & Tan, B. (2014). Regional distribution models with lack of proximate predictors: A fricanized honeybees expanding north. Diversity and Distributions, 20(2), 193-201.

Joyce, K. E., Belliss, S. E., Samsonov, S. V., McNeill, S. J., & Glassey, P. J. (2009). A review of the status of satellite remote sensing and image processing techniques for mapping natural hazards and disasters. Progress in physical geography, 33(2), 183-207.

Kumar, L., & Mutanga, O. (2018). Google Earth Engine applications since inception: Usage, trends, and potential. Remote Sensing, 10(10), 1509.

Le Conte, Y., & Navajas, M. (2008). Climate change: impact on honey bee populations and diseases. Revue Scientifique et Technique-Office International des Epizooties, 27(2), 499-510.

Makori, D. M., Fombong, A. T., Abdel-Rahman, E. M., Nkoba, K., Ongus, J., Irungu, J., ... & Landmann, T. (2017). Predicting spatial distribution of key honeybee pests in Kenya using remotely sensed and bioclimatic variables: Key honeybee pests distribution models. ISPRS International Journal of Geo-Information, 6(3), 66.

Masson-Delmotte, V., Zhai, P., Pörtner, H. O., Roberts, D., Skea, J., Shukla, P. R., ... & Waterfield, T. (2018). Global warming of 1.5 C. An IPCC Special Report on the impacts of global warming of, 1(5).

McFrederick, Q. S., Kathilankal, J. C., & Fuentes, J. D. (2008). Air pollution modifies floral scent trails. Atmospheric Environment, 42(10), 2336-2348.

McNally, A. (2018). FLDAS Noah Land Surface Model L4 Global Monthly 0.1 x 0.1 degree (MERRA-2 and CHIRPS). Greenbelt, MD, USA, Goddard Earth Sciences Data and Information Services Center (GES DISC). https://doi.org/10.5067/5NHC22T9375G

Muñoz-Sabater, J., (2019): ERA5-Land monthly averaged data from 1950 to present. Copernicus Climate Change Service (C3S) Climate Data Store (CDS). https://doi.org/10.24381/cds.68d2bb3

Nagendra, H. (2001). Using remote sensing to assess biodiversity. International journal of remote sensing, 22(12), 2377-2400.

Nemésio, A., Silva, D. P., Nabout, J. C., & Varela, S. (2016). Effects of climate change and habitat loss on a forest-dependent bee species in a tropical fragmented landscape. Insect Conservation and Diversity, 9(2), 149-160.

Nieto, A. (2014). European red list of bees.

Nightingale, J. M., Esaias, W. E., Wolfe, R. E., Nickeson, J. E., & Ma, P. L. (2008, July). Assessing honey bee equilibrium range and forage supply using satelite-derived phenology. In IGARSS 2008-2008 IEEE International Geoscience and Remote Sensing Symposium (Vol. 3, pp. III-763). IEEE.

Ogilvie, J. E., Griffin, S. R., Gezon, Z. J., Inouye, B. D., Underwood, N., Inouye, D. W., & Irwin, R. E. (2017). Interannual bumble bee abundance is driven by indirect climate effects on floral resource phenology. Ecology letters, 20(12), 1507-1515.

Rapp, J. R., Lenske, V., Solomon, E., & Young, R. (2018, December). Incorporating NASA Earth Observations into an Assessment Tool to Identify Correlations Between Factors Associated with Bee Health. In AGU Fall Meeting Abstracts (Vol. 2018, pp. GC43I-1643).

Rasmont, P., Franzén, M., Lecocq, T., Harpke, A., Roberts, S. P., Biesmeijer, J. C., ... & Schweiger, O. (2015). Climatic risk and distribution atlas of European bumblebees (Vol. 10, pp. 1-236). Pensoft Publishers.

Saha, S., Moorthi, S., Pan, H. L., Wu, X., Wang, J., Nadiga, S., ... & Goldberg, M. (2010). The NCEP climate forecast system reanalysis. Bulletin of the American Meteorological Society, 91(8), 1015-1058.

Shi, L., & Ling, F. (2021). Local Climate Zone Mapping Using Multi-Source Free Available Datasets on Google Earth Engine Platform. Land, 10(5), 454.

Schmickl, T., & Crailsheim, K. (2007). HoPoMo: A model of honeybee intracolonial population dynamics and resource management. Ecological modelling, 204(1-2), 219-245.

Schmickl, T., & Switanek, M., Crailsheim, K., Truhetz, H., & Brodschneider, R. (2017). Modelling seasonal effects of temperature and precipitation on honey bee winter mortality in a temperate climate. Science of the Total Environment, 579, 1581-1587.

Stabentheiner, A., Kovac, H., & Brodschneider, R. (2010). Honeybee colony thermoregulation–regulatory mechanisms and contribution of individuals in dependence on age, location and thermal stress. *PLoS one, 5*(1), e8967.

Steinhauer, N. A., Rennich, K., Wilson, M. E., Caron, D. M., Lengerich, E. J., Pettis, J. S., ... & Bee Informed Partnership. (2014). A national survey of managed honey bee 2012–2013 annual colony losses in the USA: results from the Bee Informed Partnership. Journal of Apicultural Research, 53(1), 1-18.

Turner, W., Spector, S., Gardiner, N., Fladeland, M., Sterling, E., & Steininger, M. (2003). Remote sensing for biodiversity science and conservation. Trends in ecology & evolution, 18(6), 306-314.

Van der Zee, R., Gray, A., Holzmann, C., Pisa, L., Brodschneider, R., Chlebo, R., ... & Wilkins, S. (2013). Standard survey methods for estimating colony losses and explanatory risk factors in Apis mellifera. Journal of Apicultural Research, 52(4), 1-36.

Vizcarra, N. (2010). Clues in the nectar. Sensing Our Planet, 34.

Wan, Z., Hook, S., Hulley, G. (2015). MOD11A1 MODIS/Terra Land Surface Temperature/Emissivity Daily L3 Global 1km SIN Grid V006 [Data set]. NASA EOSDIS Land Processes DAAC. https://doi.org/10.5067/MODIS/MOD11A1.006

Wang, L., Diao, C., Xian, G., Yin, D., Lu, Y., Zou, S., & Erickson, T. A. (2020). A summary of the special issue on remote sensing of land change science with Google earth engine. Remote Sensing of Environment, 248, 112002.

Ward, C. A., & Starks, S. A. (2000). An approach to predict Africanized honey bee migration using remote sensing. Computers & Electrical Engineering, 26(1), 33-45.

Williams, N. M., Cariveau, D., Winfree, R., & Kremen, C. (2011). Bees in disturbed habitats use, but do not prefer, alien plants. Basic and Applied Ecology, 12(4), 332-341.

Young, K. E., Abbott, L. B., Caldwell, C. A., & Schrader, T. S. (2013). Estimating suitable environments for invasive plant species across large landscapes: A remote sensing strategy using Landsat 7 ETM+. International Journal of Biodiversity and Conservation, 5(3), 122-134.

ATTACHMENTS

LIST OF ATTACHMENTS

Bound attachments:

Attachment 1   Earth observation data source table

Attachment 2   Parameter table for implementation of time series visualization

Attachment 3   EO4BEE Web Application Interface

Free attachments

Attachment 2   Poster

Attachment 3   SD card

Attachment 3   Thesis website

Structure of the SD card

Files and Folders:

Data Used for the Analysis

    ERA5_Precipitation_1950_2021_Yearly_Aggregate_EU.crf
    ERA5_Temperature_1950_2021_Yearly_Aggregate_EU.crf
    MOD11_Temperature_2001_2021_Yearly_Aggregate_CZE.crf
    TerraClimate_Precipitation_2000_2020__Yearly_Aggregate_CZE.crf

EO4BEE-HEROKU

    notebooks
        eo4bee.ipynb
    config_vars.py
    Procfile
    README.md
    requirements.txt
    runtime.txt

Multidimensional PCA Results

    Temperature_1950-1985_Yearly_Aggregate_pc.crf
    Temperature_1986-2021_Yearly_Aggregate_pc.crf
    PCA_temperature_1950_1985.png
    PCA_temperature_1986_2021.png
    PCA_temperature_before-after_compare.png
    Temperature_1950-1985_Yearly_Aggregate_eigenvalues.csv
    Temperature_1950-1985_Yearly_Aggregate_loading.csv
    Temperature_1986-2021_Yearly_Aggregate_eigenvalues.csv
    Temperature_1986-2021_Yearly_Aggregate_loading.csv

Regression Analysis and Temporal Profile Analysis Results

    colony_loss_prec_trend_repre_2.xlsx
    colony_loss_temp_trend_repre_2.xlsx
    temperature_anomaly_colony_loss_repre_2.xlsx

Script for Exporting Data from GEE

export_1km_temperature_CZE.js

Script for Yearly Total Precipitation Aggregation

get_yearly_sum.ipynb

Trend Analysis Results

CZE_Precipitation_2000_2020_Yearly_Aggregate_Trend_linear.crf
CZE_Temperature_2001_2021_Yearly_Aggregate_Trend_linear.crf
EU_Precipitation_1950_2021_Yearly_Aggregate_Trend_linear.crf
EU_Temperature_1950_2021_Yearly_Aggregate_Trend_linear.crf
CZE_precip_temporal_profile.png
CZE_temp_temporal_profile.png
CZE_trend_map_precipitation.png
CZE_trend_map_temperature.png
EU_trend_map_precipitation.png
EU_trend_map_temperature.png
ZonalStats_Precipitation_Trend_Europe.xlsx
ZonalStats_Temperature_Trend_Europe.xlsx

Videos and Animations

ndvi_yearly.gif
precipitation_monthly.gif
precipitation_yearly.gif
temperature_monthly.gif
temperature_yearly.gif
monthly_avarage_temperature_2010.mp4
yearly_average_precipitation_2000_2010.mp4

MasterThesis_YuanWang.pdf

Attachment 1 –Earth observation data source table

Dataset name	Dataset provider	Spatial resolution	Time availability
MOD11A1.006 Terra Land Surface Temperature and Emissivity Daily Global 1km (Wan et al., 2015)	NASA LP DAAC at the USGS EROS Center	1000 m	2000-02-24- 2022-03-21*
TerraClimate: Monthly Climate and Climatic Water Balance for Global Terrestrial Surfaces (Abatzoglou et al., 2018)	University of California Merced	$\frac{1}{24}°$	1958-01-01 - 2020-12-01*
ERA5 Monthly Aggregates - Latest Climate Reanalysis (Hersbach et al., 2019)	ECMWF / Copernicus Climate Change Service	0.25°	1979-01-01 - 2020-06-01*
Landsat 7 Collection 1 Tier 1 8-Day NDVI Composite (Landsat-7 image courtesy of the U.S. Geological Survey)	Google	30 m	1999-01-01 - 2022-01-01*
Copernicus CORINE Land Cover	EEA/Copernicus	100 m	1986-01-0 - 2018-12-31*
FLDAS: Famine Early Warning Systems Network (FEWS NET) Land Data Assimilation System (McNally, 2018)	NASA GES DISC at NASA Goddard Space Flight Center	0.1°	1982-01-01 - 2022-02-01*
Sentinel-5P NRTI SO2: Near Real-Time Sulphur Dioxide	European Union/ESA /Copernicus	0.01°	2018-07-10 - 2022-03-28*
Copernicus Atmosphere Monitoring Service (CAMS) Global Near-Real-Time (Benedetti et al., 2009)	European Centre for Medium-Range Weather Forecasts (ECMWF)	0.4°	2016-06-21 - 2022-03-27*

*: Current time availability can be different from the one listed here since the GEE datasets might be updated.

Attachment 2 – Parameter table for implementation of time series visualization

Layer	Image Collection code	Band name	Reducer	Min	Max	Palette
Annual average temperature	MODIS/006/MOD11A1	LST_Day_1km	mean	-5	30	['040274', '040281', '0502a3', '0502b8', '0502ce', '0502e6', '0602ff', '235cb1', '307ef3', '269db1', '30c8e2', '32d3ef', '3be285', '3ff38f', '86e26f', '3ae237', 'b5e22e', 'd6e21f', 'fff705', 'ffd611', 'ffb613', 'ff8b13', 'ff6e08', 'ff500d', 'ff0000', 'de0101', 'c21301', 'a71001', '911003']
Monthly average temperature				-20	40	
Annual total precipitation	IDAHO_EPSCOR/TERRA CLIMATE	pr	sum	400	1500	['#f7fcf0', '#e0f3db', '#ccebc5', '#a8ddb5', '#7bcc4', '#4eb3d3', '#2b8cbe', '#0868ac', '#08408f']
Monthly total precipitation				0	200	
NDVI	LANDSAT/LE07/C01/T1_8DAY_NDVI	NDVI	mean	0.0	1.0	['ffffff', 'ce7e45', 'df923d', 'f1b555', 'fcd163', '99b718', '74a901', '66a000', '529400', '3e8601', '207401', '056201', '004c00', '023b01', '012e01', '011d01', '011301']
Landcover	COPERNICUS/CORINE/V20/100m	landcover	/			The "vis_params" applied for land cover is an empty object "{}"
Soil moisture (monthly/yearly mean)	NASA/FLDAS/NOAH01/C/GL/M/V001	SoilMoi00_10cm_tavg	mean	0.0	1.0	['#ffffe5', '#f7fcb9', '#d9f0a3', '#addd8e', '#78c679', '#41ab5d', '#238443', '#006837', '#004529']
PM 2.5 (monthly/yearly mean)	ECMWF/CAMS/NRT	particulate_matter_d_less_than_25_um_surfac	mean	0.0	7.6e-08	["5e4fa2", "3288bd", "66c2a5", "abe0a4", "e6f598", "ffffbf", "fee08b", "fdae61", "f46d43", "d53e4f", "9e0142"]
Sulphur Dioxide (monthly/yearly mean)	COPERNICUS/S5P/NRTI/L3_SO2	SO2_column_number_density	mean	0.0	0.0005	['black', 'blue', 'purple', 'cyan', 'green', 'yellow', 'red']

Attachment 3 – EO4BEE Web Application Interface